CHAPTER 8

Low Noise Amplifier Design

CHAPTER OUTLINE

Low noise amplifier is located at the front-end of a receiver and plays the role of amplifying weak received signals. As shown in Fig. 8.1, the signal (P_S) is not the only signal present at the input, also present is the noise (N_S) which is likewise amplified together with the signal. In addition, the contributions of internal noise sources of the active device, used in the amplifier, also appear at the output. As a result, the signal to noise ratio becomes worse at the output than was received at the input. Thus, the low noise amplifier adds only a minimum of output noise and amplifies the signal to the extent that the next stage signal processing components can process the signal although this is achieved at some cost to signal to noise ratio.

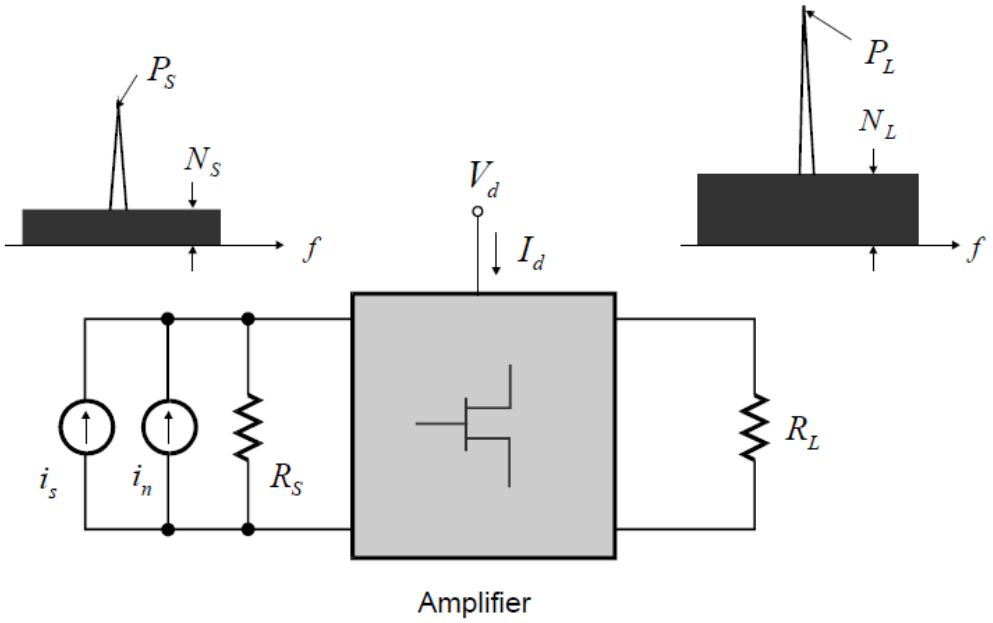

Figure 8.1 Low noise amplifier design concept

Two well known methods for designing low-noise amplifiers are (1) using the equivalent circuit of the active device employed in the amplifier and (2) using the measured S-parameters of the active device. As we have seen previously, in general, high-frequency active devices, including even semiconductor chips, are very complex, which is why the equivalent circuit design method is not commonly used. Low noise amplifiers are mostly designed using the measured S-parameters and noise parameters of the active device at a given DC bias. This design method is fairly mathematical and has been well developed from the past. However the disadvantage is that the frequency-dependent statistical variation of the S-parameters used in the design cannot be predicted and so the changes in amplifier characteristics are consequently somewhat difficult to predict. That is, during large-scale production, their accuracy is more difficult to predict compared to models and the tolerance of the designed amplifier is also difficult to predict. However, despite these shortcomings, the design with measured parameters is fairly systematic; and is possible even without knowing the details of the active device. The ease of predicting the amplifier characteristics is also an advantage.

The design of typical low noise amplifier using measured parameters as shown in Fig. 8.2, comes down to the determination of the impedance looking into the load and source from the active device.

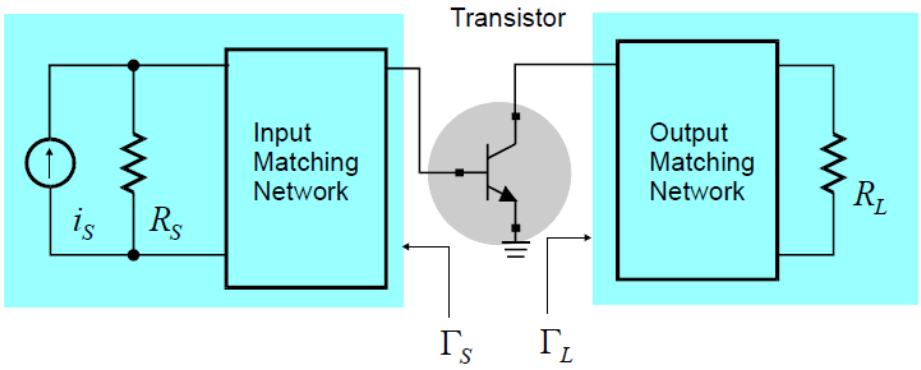

Figure 8.2 The reflection coefficient looking into the source and load from the active device.

In this chapter, we shall explain the gain, which is an important measure of a low noise amplifier, as a function of the source and load reflection coefficients, Γ_S and Γ_L shown in Fig. 8.2; and we shall also look at the Γ_S and Γ_L giving optimum gain from design perspective. In addition, the gain degradation due to the choice of impedance at the input other than the optimum Γ_S and Γ_L will be examined. In designing low noise amplifier, not only the gain must be taken into consideration, but so must the noise; which is the changes in noise figure when a load or source is connected to an active device, already examined in Chapter 4. In this chapter, we will consider the noise figure and gain as well as optimum design method of low-noise amplifier.

Furthermore, because the active device being used has some inherent degree of feedback, it shows negative resistance for specific Γ_S and Γ_L; due to which the amplifier can turn into an oscillator. Therefore, the problem of determining whether the active device will offer a negative resistance at a given frequency; and the method of stabilizing in that case will be explored.

8.1 GAINS

8.1.1 Input and Output Reflection Coefficients Definition

In order to determine the gain which depends on the load and source impedances connected to the active device, the input and output reflection coefficients must be defined. This is shown in Fig. 8.3. The general source and load impedances are fixed as $R_S=R_L=Z_o$. These impedances are converted into the appropriate impedances through the matching circuit to derive optimum performance from the active device. Γ_S represents the reflection coefficient looking into the input matching circuit from the active device; while the reflection coefficient looking into the load side of the active device is denoted as Γ_L. Note that, the reference impedance is required in order to measure these reflection coefficients; which are the same as the measurement reference impedance when measuring the S-parameters of active devices.

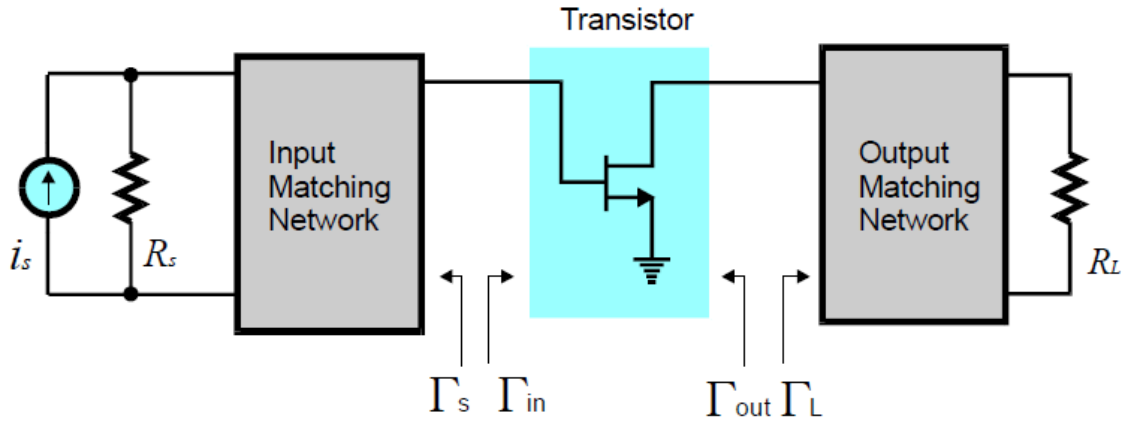

Figure 8.3 Definition of reflection coefficients

The reflection coefficient looking into the active device from the input when a load Γ_L is connected to the active device is denoted as Γ_{in}; and similarly, the reflection coefficient looking into the output of the active device is denoted as Γ_{out} when a source Γ_S is connected to the active device. Therefore, using the S-parameters of the active device, these reflection coefficients are expressed as:

$$\Gamma_{in} = S_{11} + \frac{S_{12}S_{21}\Gamma_L}{1 - S_{22}\Gamma_L}, \tag{8.1}$$

$$\Gamma_{out} = S_{22} + \frac{S_{12}S_{21}\Gamma_s}{1 - S_{11}\Gamma_s}. \tag{8.2}$$

8.1.2 Thevenin Equivalent Circuit

Figure 8.4 shows a circuit for measuring the reflection coefficient of a Thevenin equivalent circuit. The Thevenin equivalent circuit is shown in the shaded area, having voltage source E_T and internal impedance Z_T. The port is connected to the Thevenin equivalent circuit for measuring the reflection coefficient. Here, E_o and Z_o represent the port voltage and impedance respectively.

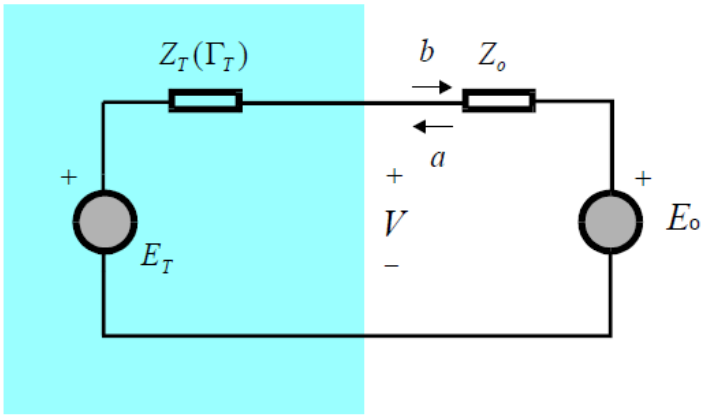

Figure 8.4 Thevenin equivalent circuit

Then, the voltage V in Fig. 8.4 is determined by superposition as:

$$V = E_o \frac{Z_T}{E_o + Z_T} + E_T \frac{Z_o}{Z_o + Z_T} = V^+ + V^- \quad , \tag{8.3}$$

which is the sum of the incident and reflected voltages as indicated in equation (8.3). The incident voltage is:

$$V^+ = \frac{E_o}{2} . \tag{8.4}$$

Therefore, substituting equation (8.4) into (8.3), the reflected voltage V^- from equation (8.3) is given by:

$$V^- = V^+ \frac{Z_T - Z_o}{Z_T + Z_o} + E_T \frac{Z_o}{Z_o + Z_T} \quad , \tag{8.5}$$

Expressing these voltages in terms of normalized incident and reflected voltages a and b;

$$b = \frac{V^-}{\sqrt{2Z_o}} = \Gamma_T a + b_T \, , \tag{8.6}$$

$$b_T = \frac{E_T}{\sqrt{2}} \frac{\sqrt{Z_o}}{Z_o + Z_T} . \tag{8.7}$$

The reflected voltage in equation (8.6) consists of two terms. The first term is the reflection coefficient looking into Thevenin circuit when E_T=0. The second term is the reflection coefficient which depends on the voltage source E_T. This can be interpreted as the voltage appearing across the port impedance Z_o when E_o=0, which is simply a load without source. In circuit theory, E_T of the

Thevenin equivalent circuit of a 1-port is found by measuring open circuit voltage. Similarly the impedance Z_T, is obtained by measuring the 1-port impedance with all the internal sources in the 1-port turned off. The reflection coefficient given by (8.6) resembles such circuit theory. The reflection coefficient Γ_T is obtained by measuring the reflection coefficient with the source E_T turned off. Similarly, the reflection coefficient due to the source E_T is found by measuring the voltage delivered to the port impedance instead of measuring the open circuit voltage. The sum of these constitutes the total reflection given of (8.6). The difference is in measuring the internal source contributions by using a Z_o termination instead of open circuit.

■ Example 8.1

Prove that, $|b_T|^2$ obtained from equation (8.7) when E_o=0 is the power delivered to the source resistance, Z_o.

Solution

$$|b_T|^2 = \frac{1}{2} Z_o \frac{|E_T|^2}{|Z_o + Z_T|^2},$$

Since

$$P_L = \frac{1}{2} Z_o |I_L|^2 = \frac{1}{2} Z_o \left| \frac{E_T}{Z_o + Z_T} \right|^2 = |b_T|^2,$$

it can be seen that $P_L = |b_T|^2$.

■

Next, we examine the power delivered to the load when a Thevenin equivalent circuit is connected to a load Γ_L as shown in Fig. 8.5. Note that all the reflection coefficients are measured with the same reference impedance Z_o.

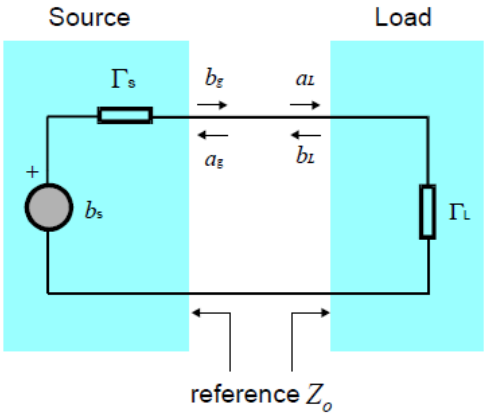

Figure 8.5 Source and load connected circuit

The reflected voltage towards the load in Fig. 8.5 is

$$b_g = \Gamma_s a_g + b_s, \tag{8.8}$$

while the load reflected voltage is

$$b_L = \Gamma_L a_L; \tag{8.9}$$

and since $b_g=a_L$ and $a_g=b_L$, the incident voltage toward the load can be obtained from the two equations as:

$$a_L = \frac{b_s}{1-\Gamma_s\Gamma_L} \quad , \tag{8.10}$$

Thus, the power delivered to the load is

$$P_L = |a_L|^2 - |b_L|^2 = |a_L|^2\left(1-|\Gamma_L|^2\right). \tag{8.11}$$

Substituting equation (8.10) into (8.11), P_L can be expressed as:

$$P_L = \frac{|b_s|^2\left(1-|\Gamma_L|^2\right)}{|1-\Gamma_s\Gamma_L|^2}. \tag{8.12}$$

In addition, available power from the source is obtained when the source and the load are conjugate matched; that is when $\Gamma_S=(\Gamma_L)^*$; substituting this condition into equation (8.12);

$$P_A = \frac{|b_s|^2}{1-|\Gamma_s|^2}. \tag{8.13}$$

In order to verify that, the result given by (8.13) is the available power, equation (8.7) is substituted into (8.13),

$$P_A = \frac{|b_s|^2}{1-|\Gamma_s|^2} = \frac{\left(\frac{E_T}{\sqrt{2}}\frac{\sqrt{Z_o}}{Z_o+Z_s}\right)}{1-\left(\frac{Z_s-Z_o}{Z_s+Z_o}\right)^2} = \frac{E_T^2}{8Z_s}. \tag{8.14}$$

It can be seen that, this result is the same as the available power that can be obtained from the source having internal resistance Z_S. Also, the ratio of power delivered to the load to available power can be computed as:

$$G = \frac{P_L}{P_A} = \frac{\left(1-|\Gamma_s|^2\right)\left(1-|\Gamma_L|^2\right)}{|1-\Gamma_s\Gamma_L|^2}. \tag{8.15}$$

8.1.3 Power Gains

Amplifier gain is one of the key performance indicators and is defined in many ways based on measurement and design. Among them is the transducer power gain which is frequently used in measurement, defined as:

$$G_T = \frac{\text{Delivered Power to Load}}{\text{Available Power from Source}}. \tag{8.16}$$

In measuring this gain, the available power from a source with 50 ohm internal resistance is measured by connecting a power meter (of 50 ohm internal resistance) to the source. Then, inserting the amplifier between them and measuring the delivered power to the power meter, the ratio of the powers can be obtained to determine the transducer gain given by (8.16). On the other hand, from design perspective, when the output impedance of the amplifier is conjugate matched by varying the load as shown in Fig. 8.6, the available power at the output can be obtained. The ratio of the available output power to the available power from the input is called available power gain which is defined as follows:

$$G_A = \frac{\text{Available Power from Output}}{\text{Available Power from Source}}. \tag{8.17}$$

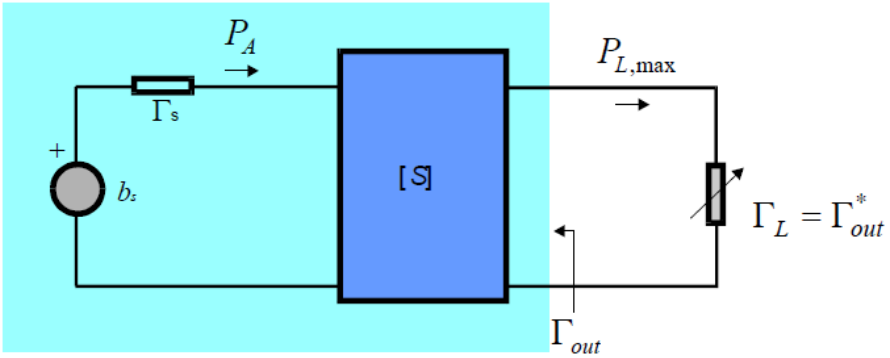

Figure 8.6 The concept of available power gain

This is the maximum gain derived from the output for a given source resistance, which is a function of only the source resistance. Therefore, this represents the degradation of the gain due to fixed source impedance.

In contrast, for a fixed load, based on the symmetrical concept shown in Fig. 8.7, when the input impedance is adjusted to deliver maximum power to the load, then the ratio of input power to output power is called power gain. This is defined as follows:

$$G_p = \frac{\text{Delivered Power to Load}}{\text{Input Power at Device Input}}. \tag{8.18}$$

This gain, as an indicator of the degradation of the gain due to fixed load, is commonly used in design. The previous power gains can be expressed in terms of the 2-port S-parameters, input and output impedances using the method described in the previous section; this will be discussed in the next chapter.

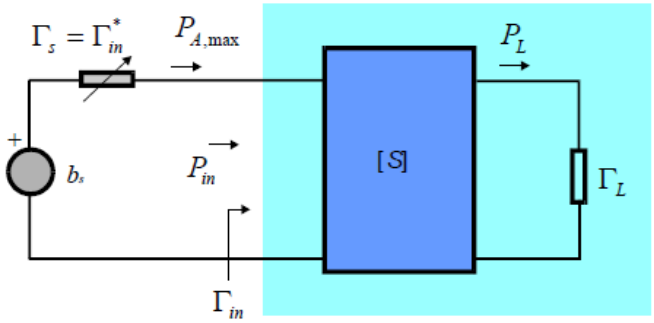

Figure 8.7 The concept of power gain

8.1.3.1 Transducer Power Gain

Figure 8.8(a) depicts an amplifier configured with an active device as well as input and output matching circuits, while Fig. 8.8(b) shows a representation of the same circuit with a simplified input and output at the device plane. The input may be represented by a Thevenin equivalent circuit, while the output can be be represented by a single load.

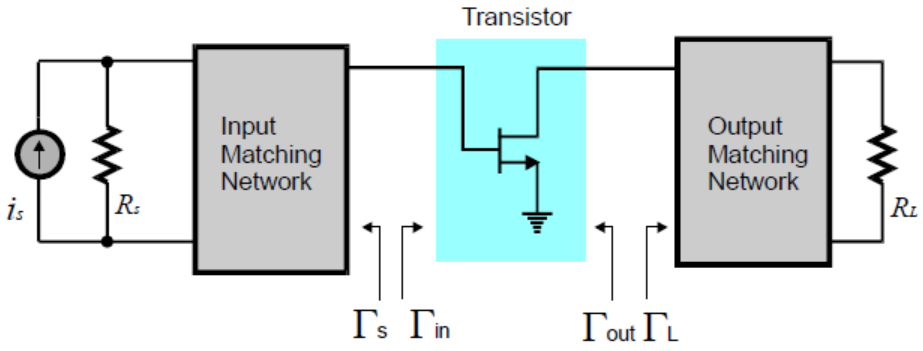

(a)

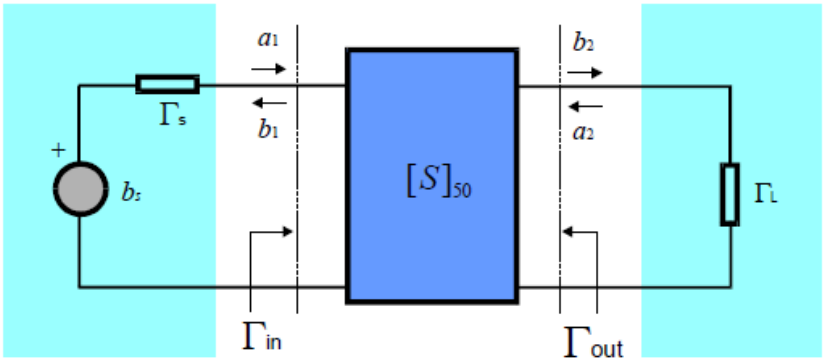

(b)

Figure 8.8 (a) Block diagram of amplifier, and (b) its equivalent circuit

Representing the 1-port circuit seen from the load Γ_L, which includes the active device [S] and the input circuit in Fig. 8.9, by the Thevenin equivalent circuit, the Thevenin resistance Γ_L becomes:

$$\Gamma_T = \Gamma_{out}\,. \tag{8.19}$$

Also the Thevenin reflected voltage b_T is the voltage appearing across the load Z_o when the load Γ_L is replaced by Z_o. From Fig. 8.9, b_T is given by

$$b_T = b_2\big|_{a_2=0} = S_{21}a_1\,. \tag{8.20}$$

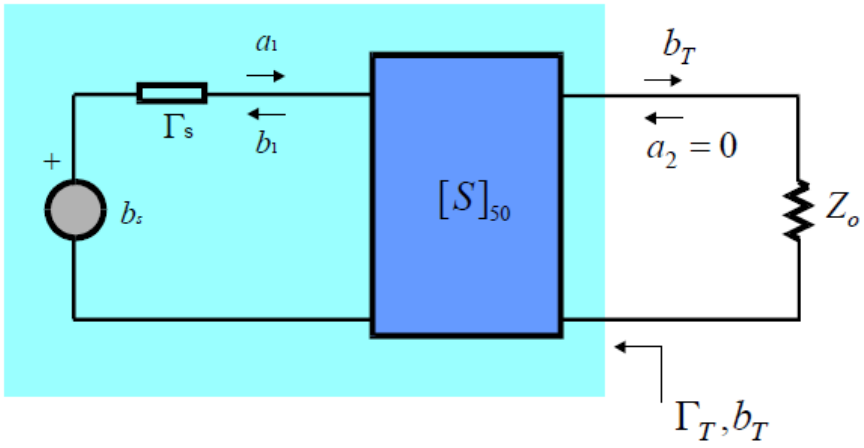

Figure 8.9 Thevenin equivalent circuit analysis

Note that $\Gamma_{in}=S_{11}$ because $a_2=0$. Applying equation (8.10), a_1 is given by

$$a_1 = \frac{b_s}{1 - S_{11}\Gamma_s}, \tag{8.21}$$

Thus, from (8.20), Thevenin reflected voltage b_T is

$$b_T = S_{21}\frac{b_s}{1 - S_{11}\Gamma_s}. \tag{8.22}$$

Therefore, the equivalent circuit seen from the load Γ_L can be represented as shown in Fig. 8.10.

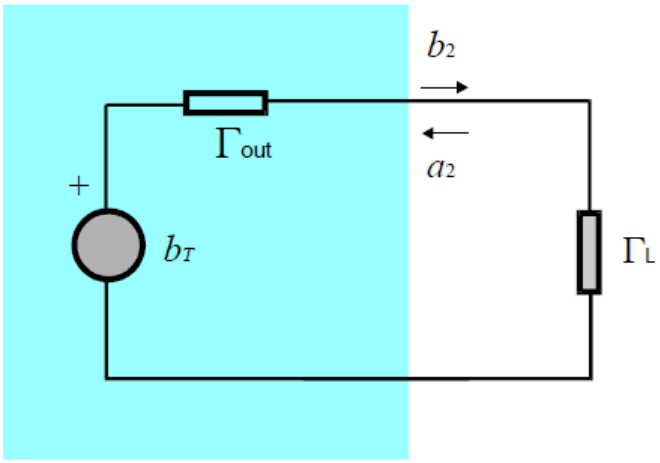

Figure 8.10 Thevenin equivalent circuit seen from the load

Applying equation (8.12), the power delivered to the load Γ_L is

$$P_L = \frac{|b_T|^2\left(1 - |\Gamma_L|^2\right)}{|1 - \Gamma_{out}\Gamma_L|^2} = |b_s|^2 \frac{|S_{21}|^2}{|1 - S_{11}\Gamma_s|^2}\frac{\left(1 - |\Gamma_L|^2\right)}{|1 - \Gamma_{out}\Gamma_L|^2}. \tag{8.23}$$

Since the available power from the source is the same as in equation (8.13), the transducer power gain G_T is expressed as

$$G_T = \frac{P_L}{P_A} = \frac{1 - |\Gamma_s|^2}{|1 - S_{11}\Gamma_s|^2}|S_{21}|^2\frac{1 - |\Gamma_L|^2}{|1 - \Gamma_{out}\Gamma_L|^2}, \tag{8.24}$$

Expressed in a different way, the transducer gain can be computed using the reflection coefficient at the input of the active device and the Thevenin equivalent circuit of the input, from which the following result can be obtained:

$$G_T = \frac{P_L}{P_A} = \frac{1-|\Gamma_s|^2}{|1-\Gamma_{in}\Gamma_s|^2}|S_{21}|^2 \frac{1-|\Gamma_L|^2}{|1-S_{22}\Gamma_L|^2}. \tag{8.25}$$

This is the same result as in equation (8.24), only that it is expressed in a different way.

8.1.3.2 Available Power Gain

Available power gain is defined as the ratio of available power at the device input to available power at the output. This can be obtained using the previously derived transducer power gain. Note that the transducer power gain is defined in terms of the available power at the input and the delivered power to the output load; however, the available power at the output is the available power when the output impedance is conjugate matched to Γ_{out} as shown in Fig. 8.11. This condition is $\Gamma_L=(\Gamma_{out})^*$. Since the power delivered to the load is the available power at the output, the available power gain can be obtained by substituting $\Gamma_L=(\Gamma_{out})^*$ into the transducer gain in equation (8.24). Therefore the available power gain is given by

$$G_T = \frac{P_L}{P_A} = \left.\frac{\left(1-|\Gamma_s|^2\right)|S_{21}|^2\left(1-|\Gamma_L|^2\right)}{|1-\Gamma_{out}\Gamma_L|^2|1-S_{11}\Gamma_s|^2}\right|_{\Gamma_L=\Gamma_{out}^*} = \frac{\left(1-|\Gamma_s|^2\right)|S_{21}|^2}{|1-S_{11}\Gamma_s|^2\left(1-|\Gamma_{out}|^2\right)}. \tag{8.26}$$

This can also be interpreted as the maximum gain for fixed Γ_S.

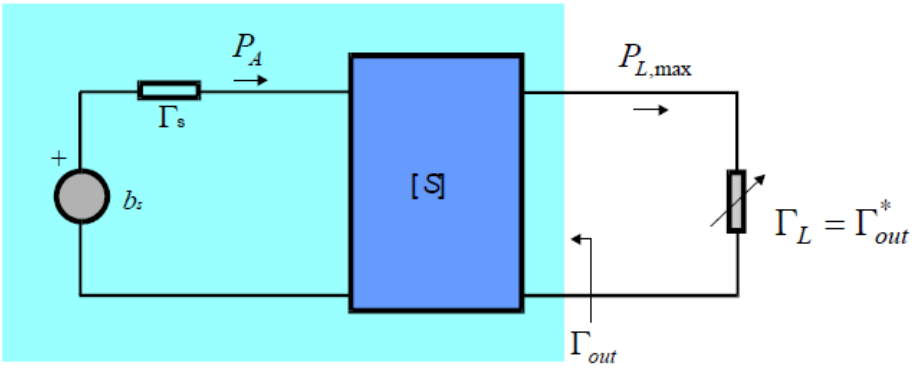

Figure 8.11 Diagram for calculating available power gain

8.1.3.3 Power Gain

The power Pin delivered to the input of the active device as shown in Fig. 8.12 is given by:

$$P_{in} = |a_1|^2 - |b_1|^2 = |a_1|^2\left(1-|\Gamma_{in}|^2\right), \tag{8.27}$$

Using equation (8.10), this results in

$$P_{in} = \frac{|b_s|^2 \left(1 - |\Gamma_{in}|^2\right)}{|1 - \Gamma_{in}\Gamma_s|^2}. \tag{8.28}$$

In addition, a_1 and a_2 in Fig. 8.12 are given by:

$$a_1 = \frac{b_s}{1 - \Gamma_{in}\Gamma_s} \quad , \tag{8.29}$$

$$a_2 = \Gamma_L b_2 \, . \tag{8.30}$$

which if substituted in b_2 gives:

$$b_2 = S_{21}a_1 + S_{22}a_2 = S_{21}\frac{b_s}{1 - \Gamma_{in}\Gamma_s} + S_{22}\Gamma_L b_2 \, . \tag{8.31}$$

Then b_2 can be computed as

$$b_2 = \frac{S_{21}b_s}{\left(1 - \Gamma_{in}\Gamma_s\right)\left(1 - S_{22}\Gamma_L\right)} . \tag{8.32}$$

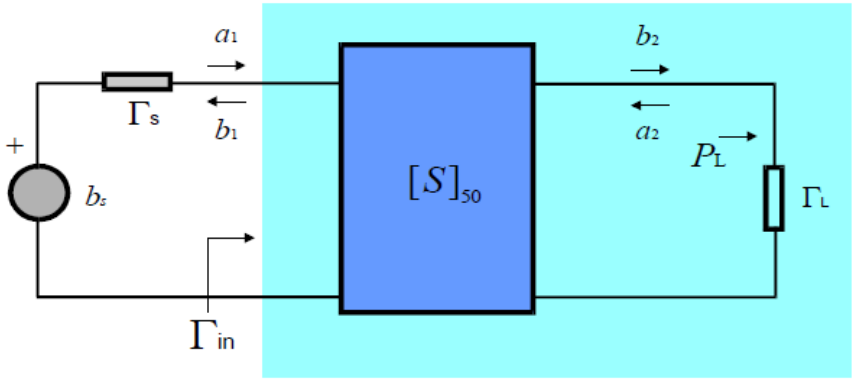

Figure 8.12 Thevenin equivalent circuit analysis for the calculation of power gain

Thus, the power delivered to the load is given by:

$$P_L = |b_2|^2 \left(1 - |\Gamma_L|^2\right) = |b_s|^2 \frac{|S_{21}|^2}{|1 - \Gamma_{in}\Gamma_s|^2} \frac{\left(1 - |\Gamma_L|^2\right)}{|1 - S_{22}\Gamma_L|^2} . \tag{8.33}$$

Therefore, based on the definition of power gain, the ratio of the input power P_{in} to power delivered to the load P_L is given by

$$G_P = \frac{P_L}{P_{in}} = \frac{|S_{21}|^2\left(1-|\Gamma_L|^2\right)}{\left(1-|\Gamma_{in}|^2\right)\left(1-S_{22}|\Gamma_L|^2\right)}. \tag{8.34}$$

The power gain is the ratio of input power to the power delivered to the load. However this put another way, the source impedance must be conjugate matched to the input impedance so that maximum power is delivered to the input of the active device. The ratio of this input power to the power delivered to the load leads to the same result given by (8.34). This is found in the exercises; and the same result is obtained with such analysis. Another way of interpreting this is, it represents the maximum gain of the active device for a fixed load Γ_L.

8.1.3.4 Unilateral Gain

In general, because the active device has some feedback, $S_{12}\neq 0$. However, this can typically be made 0 by adding the appropriate feedback circuit in which case, there will be no feedback from output to input. This is then said to be unilateral. The resulting gain is called Mason's gain, U which is expressed as follows:

$$U = \frac{\left|\frac{S_{21}}{S_{12}}-1\right|^2}{2k\left|\frac{S_{21}}{S_{12}}\right| - 2\,\mathrm{Re}\left(\frac{S_{21}}{S_{12}}\right)}, \tag{8.35a}$$

$$k = \frac{1-|S_{11}|^2-|S_{22}|^2+|D|^2}{2|S_{12}S_{21}|}. \tag{8.35b}$$

Since the Mason's gain is the gain measured after the active device has been absolutely stabilized by removing feedback, this can be seen as the true gain of the active device. Therefore, it is used as criteria to determine whether a measured device at an arbitrary frequency is active or passive using measured S- parameters.

As an approximate expression to this, $S_{12}=0$ is substituted into equation (8.35a), since S_{12} which represents the feedback from output to input is generally less than 1. This results in the transducer power gain for $S_{12}=0$. In this case, since $\Gamma_{in}= S_{11}$ and $\Gamma_{out}= S_{22}$, the transducer power gain is expressed as:

$$G_{TU} = G_T\big|_{S_{12}=0} = \frac{\left(1-|\Gamma_s|^2\right)|S_{21}|^2\left(1-|\Gamma_L|^2\right)}{|1-S_{11}\Gamma_s|^2\,|1-S_{22}\Gamma_L|^2}. \tag{8.36}$$

When the input and output reflection coefficients are each conjugate matched ($\Gamma_S=(\Gamma_{in})^*$, $\Gamma_L=(\Gamma_{out})^*$), maximum gain is then obtained and the unilateral gain $G_{TU,max}$ is

$$G_{TU,\max} = \frac{|S_{12}|^2}{\left(1-|S_{22}|^2\right)\left(1-|S_{11}|^2\right)}. \tag{8.37}$$

The calculation of this unilateral gain is simple compared to other gains and was commonly used in the past to evaluate the maximum gain of active devices when computers were not prevalent.

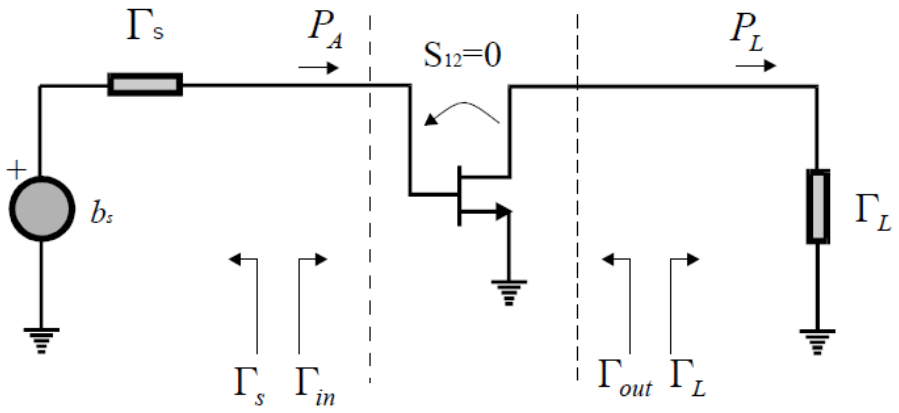

Figure 8.13 Unilateral gain

8.2 STABILITY AND CONJUGATE MATCHING

Active devices generally have feedback from output to input; for a load which offers negative resistance at the input, there is the possibility of oscillation and similarly a negative resistance can appear at the output for a specified source resistance. Such a negative resistance does not necessarily cause oscillation, but it limits the matching of the amplifier and must be eliminated through stabilization method. Also, when stabilizing, the maximum gain point appears at the conjugate matching point, and this conjugate matching point is derived mathematically; the characteristics of which will be examined in this chapter.

8.2.1 Load and Source Stability Regions

A particular load or source impedance offers negative resistance to the input and output impedances of the active device, so the region of a specified load and source impedance will first have to be known. When a negative resistance is induced at the input or output of an active device, the magnitude of input or output reflection coefficients are mathematically greater than 1. That is, $|\Gamma_{in}|>1$ or so is $|\Gamma_{out}|>1$. Therefore, in order to know the stability region, the problem reduces to finding:

1) A region of Γ_L which gives $|\Gamma_{in}|\leq 1$ and
2) A region of Γ_S which gives $|\Gamma_{out}|\leq 1$

Condition 1) limits the range of load selection which is why it is called load stability circle and Condition 2) limits the range of source selection and is thus called source stability circle. After

determining the locus of the boundary region ($|\Gamma_{in}|=1$ and $|\Gamma_{out}|=1$), the locus divides a region of Γ_S into two regions. Once a stability region is found between these two regions, the remaining area becomes automatically unstable; that is a region giving rise to negative input or output resistances. From Fig. 8.14, the input reflection coefficient is

$$\Gamma_{in} = S_{11} + \frac{S_{12}S_{21}\Gamma_L}{1-S_{22}\Gamma_L} = \frac{S_{11}-D\Gamma_L}{1-S_{22}\Gamma_L}. \tag{8.38}$$

where $D=S_{11}S_{22}-S_{21}S_{12}$

When a negative resistance does not appear in Γ_{in}, this results in a region of $|\Gamma_{in}|\leq 1$, however in order to find the Γ_L which gives the locus of the circle of the boundary line $|\Gamma_{in}|=1$, equation (3.38) is expressed in terms of Γ_L, giving:

$$|\Gamma_{in}| = \left|\frac{S_{11}-D\Gamma_L}{1-S_{22}\Gamma_L}\right| = 1. \tag{8.39}$$

Multiplying both sides of the equation by $|S_{22}/D|$ and arranging, the following expression is obtained.

$$\left|\frac{\Gamma_L - \frac{S_{11}}{D}}{\Gamma_L - \frac{1}{S_{22}}}\right| = \left|\frac{S_{22}}{D}\right|. \tag{8.40}$$

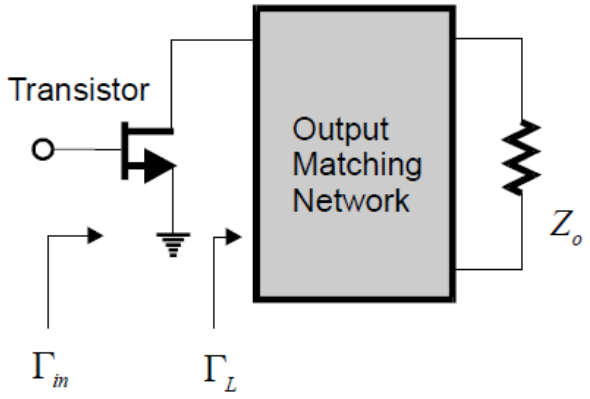

Figure 8.14 Load stability

Simplifying each term of equation (8.40),

$$\left|\frac{\Gamma_L - A}{\Gamma_L - B}\right| = m. \tag{8.41}$$

where A and B represent two points on the Γ_L plane and are expressed as follows:

$$A = \frac{S_{11}}{D} = \frac{S_{11}D^*}{|D|^2},$$

$$B = \frac{1}{S_{22}} = \frac{S_{22}^*}{|S_{22}|^2}.$$

From (8.41), m represents the ratio of the distances from an arbitrary point in the Γ_L plane to two points *A* and *B*. This locus is well known to be a circle as shown in Fig. 8.15. The internal (I) and external (E) division points with the division ratio m:1 can be obtained from two points *A* and *B*. The center of the circle becomes their mid-point between *I* and *E*. The half of the distance between points I and E becomes the radius of the circle.

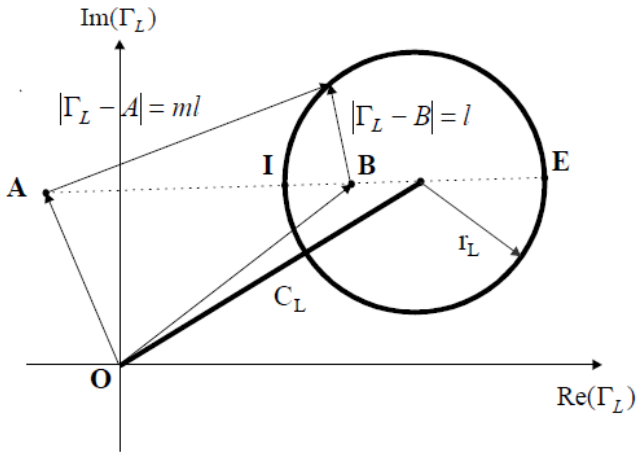

Figure 8.15 Locus of $|\Gamma_{in}|=1$ in the Γ_L plane

The internal and external division points are thus determined as:

$$I = \frac{mB + A}{m+1},$$

$$E = \frac{mB - A}{m-1}.$$

The center of the circle C_L and radius r_L are then determined from the internal and external division points as

$$C_L = \frac{I+E}{2} = \frac{m^2B - A}{m^2 - 1}, \tag{8.42a}$$

$$r_L = \left|\frac{E-I}{2}\right| = \left|\frac{m(B-A)}{m^2-1}\right|. \tag{8.42b}$$

Substituting A, B and m into the above equations, the center of the circle C_L and radius r_L in the Γ_L plane are given by:

$$C_L = \frac{S_{22}^* - D^* S_{11}}{|S_{22}|^2 - |D|^2}, \tag{8.43a}$$

$$r_L = \frac{|S_{12}S_{21}|}{\left||S_{22}|^2 - |D|^2\right|}. \tag{8.43b}$$

Load stability circles drawn using the described results are as shown in Fig. 8.16. In order to determine the region of stability between the two regions divided by the load stability circle, setting Γ_L=0 results in the input reflection coefficient Γ_{in}=S_{11}. Therefore, $|S_{11}|$<1 implies $|\Gamma_{in}|\leq 1$ for Γ_L=0; the stable region becomes the region inside the unit Smith chart circle including the origin as shown in Fig. 8.16(a). On the other hand, since $|\Gamma_{in}|$>1 for $|S_{11}|$>1 when Γ_L=0, the region that includes the origin becomes unstable.

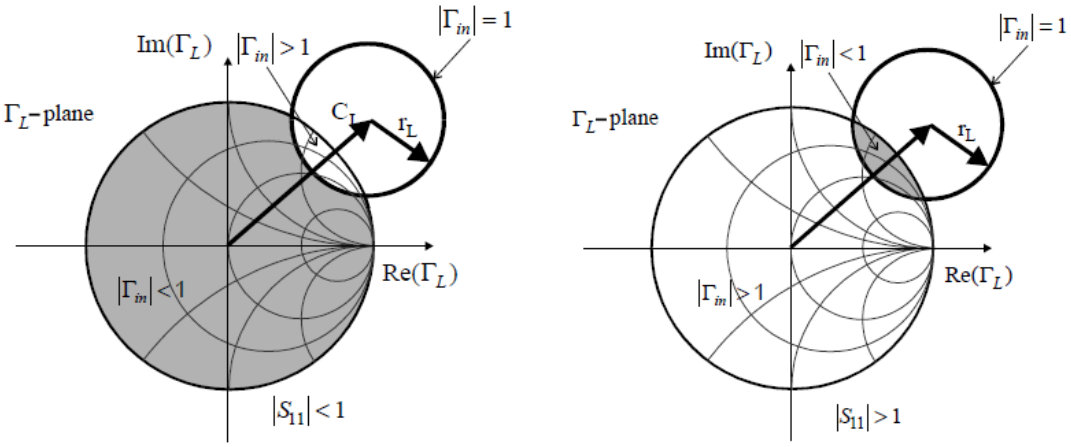

(a) (b)

Figure 8.16 Stable region in the Γ_L plane: (a) when $|S_{11}|$<1 (b) when $|S_{11}|$>1

Similarly, in order to determine the region of the source reflection coefficient giving a stable output reflection coefficient, the output reflection coefficient Γ_{out} in Fig. 8.17 is expressed as

$$\Gamma_{out} = S_{22} + \frac{S_{12}S_{21}}{1-S_{11}\Gamma_s} = \frac{S_{22} - D\Gamma_s}{1-S_{11}\Gamma_s} \tag{8.44}$$

If Γ_{out} is set to $|\Gamma_{out}|=1$ and the source stability circles are obtained, since the result will be the same as interchanging the subscript 1 and 2 in equation (8.38), the subscript 1 and 2 in equation (8.43) are interchanged for the source stability circles. Therefore, the center C_S and radius r_S of the circle giving $|\Gamma_{out}|=1$ in the Γ_S plane are giving by:

$$C_s = \frac{S_{11}^* - D^* S_{22}}{|S_{11}|^2 - |D|^2}, \tag{8.45a}$$

$$r_s = \frac{|S_{12}S_{21}|}{\left||S_{11}|^2 - |D|^2\right|}. \tag{8.45b}$$

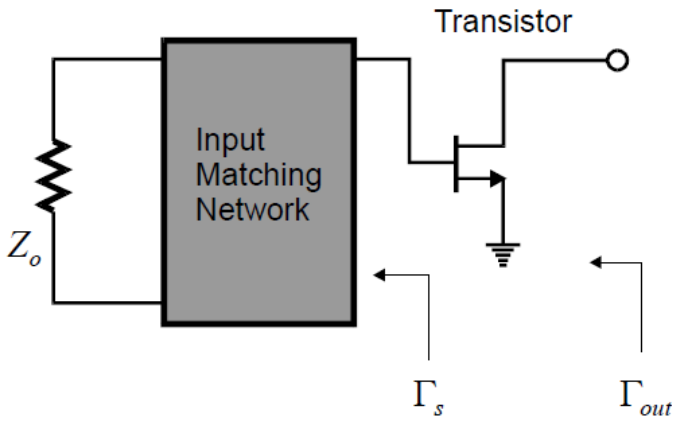

Figure 8.17 Source stability

The stability circles drawn with this center and radius are shown in Fig. 8.18 and, for the same reason as in the case of the load stability circle, when $|S_{22}|<1$, the region inside unit Smith chart including the origin represents the stability region as shown in Fig. 8.18(a). Similarly, when $|S_{22}|>1$, the region including the origin becomes the unstable region.

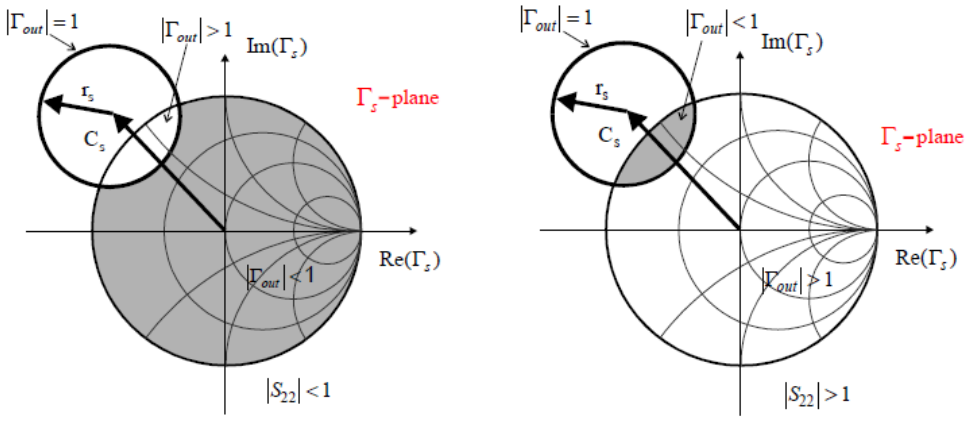

Figure 8.18 Stable region in the Γ_S plane: (a) when $|S_{22}|<1$ (b) when $|S_{22}|>1$

8.2.2 Stability Factor

As can be seen from Figs. 8.16 (a) and 8.18 (a), when equations (8.46) and (8.47) are satisfied, the circles appear as shown in Fig. 8.18 and the region of the Smith chart where Γ_S and Γ_L are less than 1 are always the region of stability. Therefore equations (8.46) and (8.47) are the necessary and sufficient conditions for stability.

$$\left||C_L|-r_L\right|>1 \quad \text{for } |S_{11}|<1, \tag{8.46}$$

$$\left||C_S|-r_S\right|>1 \quad \text{for } |S_{22}|<1. \tag{8.47}$$

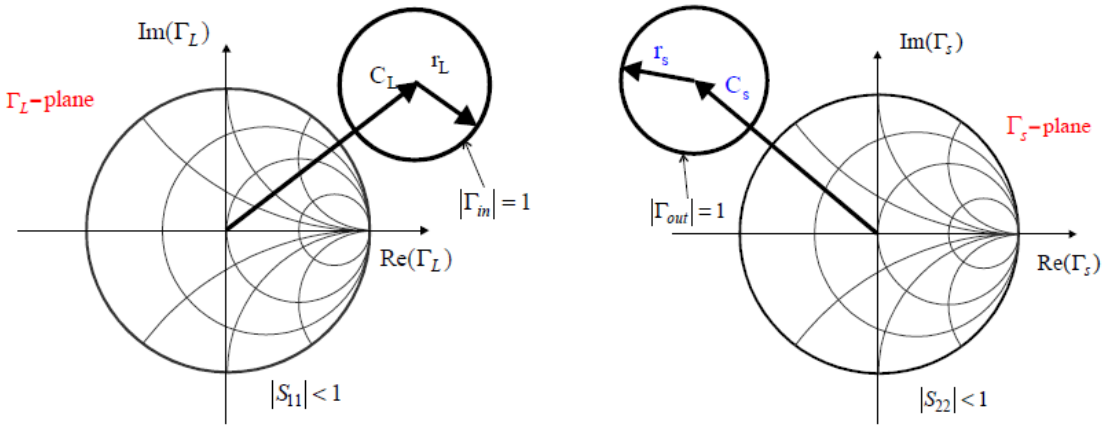

Figure 8.19 Unconditional stability: (a) Γ_L plane, (b) Γ_S plane

Substituting the obtained results of the center and radius into equation (8.46) defined above, we obtain

$$\left|\frac{\left|S_{22}-DS_{11}^{*}\right|-\left|S_{12}S_{21}\right|}{\left|S_{22}\right|^{2}-\left|D\right|^{2}}\right|>1, \tag{8.48}$$

which can also be expressed as:

$$\left\|S_{22}-DS_{11}^{*}\right|-\left|S_{12}S_{21}\right\|^{2}>\left|\left|S_{22}\right|^{2}-\left|D\right|^{2}\right|^{2}, \tag{8.49}$$

Rearranging equation (8.49), we obtain,

$$2\left|S_{12}S_{21}\right|\left|S_{22}-DS_{11}^{*}\right|<\left|S_{22}-DS_{11}^{*}\right|^{2}+\left|S_{12}S_{21}\right|^{2}-\left|\left|S_{22}\right|^{2}-\left|D\right|^{2}\right|, \tag{8.50}$$

Using the following identity in (8.51):

$$\left|S_{22}-DS_{11}^{*}\right|^{2}=\left|S_{12}S_{21}\right|^{2}+\left(1-\left|S_{11}\right|^{2}\right)\left(\left|S_{22}\right|^{2}-\left|D\right|^{2}\right). \tag{8.51}$$

Squaring each term of equation (8.50) and substituting equation (8.51) and then rearranging, equation (8.52) is obtained.

$$\left(\left|S_{22}\right|^{2}-\left|D\right|^{2}\right)^{2}\left[\left\{\left(1-\left|S_{11}\right|^{2}\right)-\left(\left|S_{22}\right|^{2}-\left|D\right|^{2}\right)\right\}^{2}-4\left|S_{12}S_{21}\right|^{2}\right]>0, \tag{8.52}$$

Thus, the necessary condition for (8.52) is

$$1-\left|S_{11}\right|^2-\left|S_{22}\right|^2-\left|D\right|^2>2\left|S_{12}S_{21}\right|. \tag{8.53}$$

Dividing both sides of (8.53) by the right hand term yields the stability factor *k*, which is used to examine the unconditional stability of 2-port circuit.

$$k=\frac{1-\left|S_{11}\right|^2-\left|S_{22}\right|^2-\left|D\right|^2}{2\left|S_{12}S_{21}\right|}>1. \tag{8.54}$$

The other condition can be considered as when the radius is large enough to include the Smith chart; which is the condition $r_L-\left|C_L\right|>1$ in (8.46). Substituting the center and radius results into this gives,

$$\left|\frac{S_{22}-DS_{11}^*}{\left|S_{22}\right|^2-\left|D\right|^2}\right|<\frac{\left|S_{12}S_{21}\right|}{\left|S_{22}\right|^2-\left|D\right|^2}-1. \tag{8.55}$$

This requires that the right-hand side be positive. Thus

$$\frac{\left|S_{12}S_{21}\right|}{\left|S_{22}\right|^2-\left|D\right|^2}>1, \tag{8.56}$$

From the stability factor,

$$2k=\frac{1-\left|S_{11}\right|^2}{\left|S_{12}S_{21}\right|}+\frac{\left|D\right|^2-\left|S_{22}\right|^2}{\left|S_{12}S_{21}\right|}>2, \tag{8.57}$$

is obtained. However, since the second term of equation (8.57) is less than 1 (from equation (8.56)), the first term must be greater than 1. Therefore,

$$1-\left|S_{11}\right|^2>\left|S_{12}S_{21}\right|, \tag{8.58}$$

which is an additional condition that must be satisfied. Likewise, from the source stability circles, the following condition is obtained.

$$1-\left|S_{22}\right|^2>\left|S_{12}S_{21}\right|. \tag{8.59}$$

In conclusion, the necessary and sufficient conditions for stability of 2-ports circuit are:

$$k>1, \tag{8.60a}$$

$$1-|S_{11}|^2 > |S_{12}S_{21}|, \tag{8.60b}$$

$$1-|S_{22}|^2 > |S_{12}S_{21}|. \tag{8.60c}$$

These are the three conditions that must be simultaneously satisfied.

■ Example 8.2

Use the 3 V 10 mA S-parameters of the FHX35LG/LP provided in ADS to determine the stability factor **k** and the frequency dependent values of the following terms:

$$\frac{1-|S_{11}|^2}{|S_{12}S_{21}|}, \quad \frac{1-|S_{22}|^2}{|S_{12}S_{21}|}.$$

Draw the source and load stability circles at 1 GHz.

Solution
Set up the following circuit for the 2-port S-parameters of the ADS FHX35LG/LP device. Perform the simulation and enter the following equations in the Display window to verify the results.

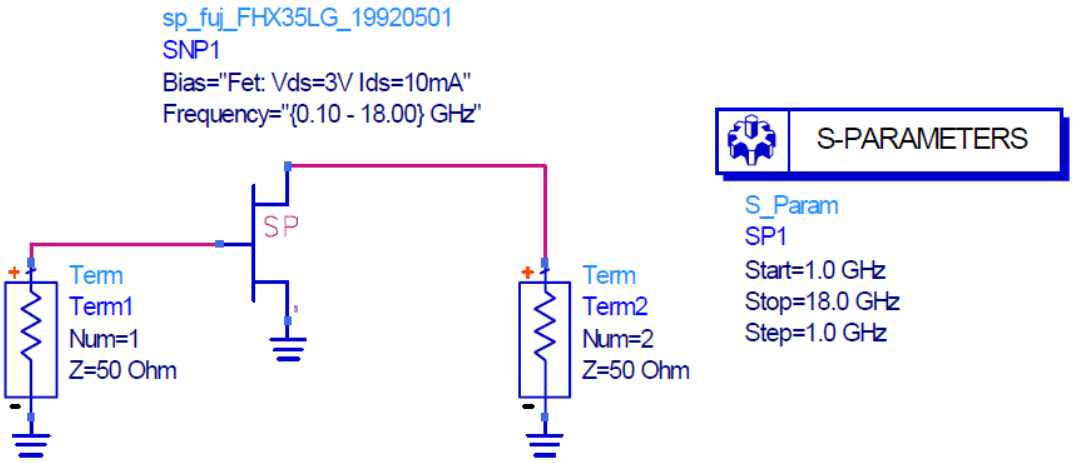

Figure 8E.1 Circuit for determining the stability of FHX35LG/LP

```
Eqn  k=stab_fact(S)
Eqn  S1=(1-(mag(S11))**2)/(mag(S12*S21))
Eqn  L1=(1-(mag(S22))**2)/(mag(S12*S21))
```

Figure 8E.2 Equations inserted in the Display window

As shown in Fig. 8E.3, because S_1 and L_1 are observed to be greater than **k**, (since the two terms are mostly greater than 1 when ***k*** is greater than 1), the stability factor **k** is critical to determining the stability. This is generally true. In addition, as can be seen from the figure, above the 12 GHz frequency, **k**>1 and it is thus stable; it is however that it becomes unstable at frequencies lower than this.

As can be verified from the results, as **k**<1 at the current frequency of 1 GHz, this is found to be the unstable frequency range. In order to find the stable region, the following equations are added in the Display window to plot the load and source stability circles at a frequency of 1 GHz

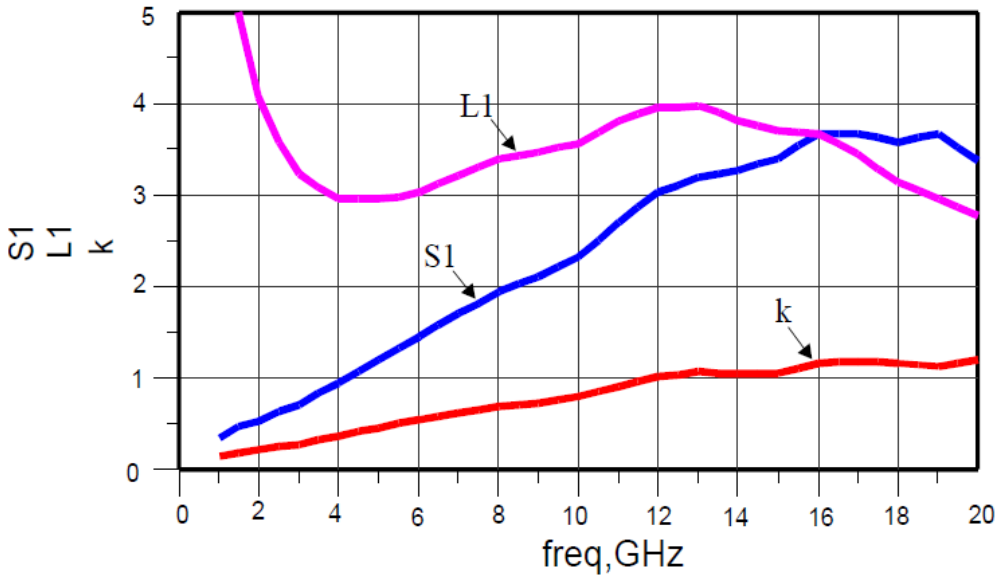

Figure 8E.3 Simulation Results

```
Eqn Source_Stability_Circle=s_stab_circle(S[0], 51)
Eqn Load_Stability_Circle=l_stab_circle(S[0],51)
```

Figure 8E.4 Equation for drawing the stability circles

The function **s_stab_circle (S[0], 51)** above is the function for drawing the source stability circle given by equation (8.45). S-parameter index for frequency is set to [0] for the selection of S-parameters at a frequency of 1 GHz. The number 51 at the end represents the number of points used in plotting the circle. Similarly, **l_stab_circle (S[0],51)** is a function for load stability circle. The circles plotted on Smith chart using these functions are as shown in Fig. 8E.5. It can be seen that, since $|S_{11}|<1$ and $|S_{22}|<1$, the region including the origin of the Smith chart is the region of stability.

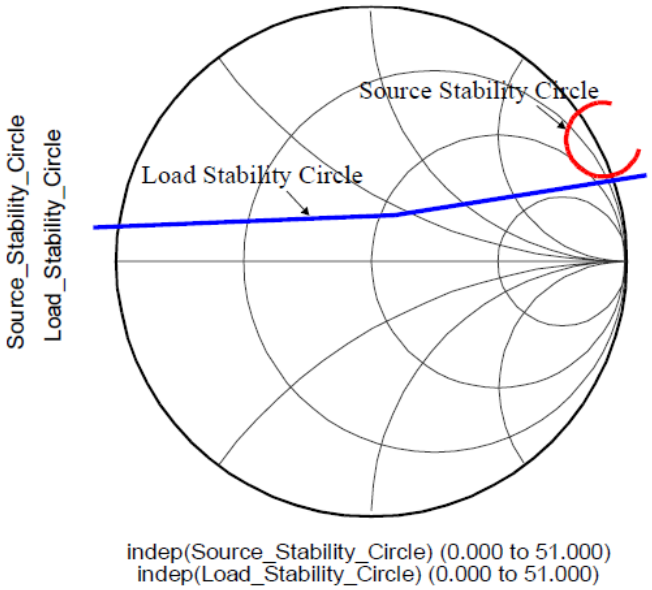

Figure 8E.5 Source and load stability circles

■

8.2.3 Conjugate Matching

Figure 8.20 shows input and output conjugate matching, the objective of which is to obtain maximum gain from the active device. In other words, by conjugate matching the input, maximum power is transferred from the source to the input of the active device. Simultaneously conjugate matching the output ensures that the maximum power that is amplified by the active device is transferred to the load. Therefore, maximum gain is obtained when the input and output are conjugate matched as follows.

$$\Gamma_{in} = S_{11} + \frac{S_{12}S_{21}\Gamma_L}{1 - S_{22}\Gamma_L} = \Gamma_s^*, \tag{8.61a}$$

$$\Gamma_{out} = S_{22} + \frac{S_{12}S_{21}\Gamma_s}{1 - S_{11}\Gamma_s} = \Gamma_L^*. \tag{8.61b}$$

The following is obtained by rearranging the above equations.

$$\left(1 - \Gamma_L S_{22}\right)\left(S_{11} - \Gamma_s^*\right) + \Gamma_L S_{12}S_{21} = 0 \tag{8.62a}$$

$$\left(1 - \Gamma_s S_{11}\right)\left(S_{22} - \Gamma_L^*\right) + \Gamma_s S_{12}S_{21} = 0 \tag{8.62b}$$

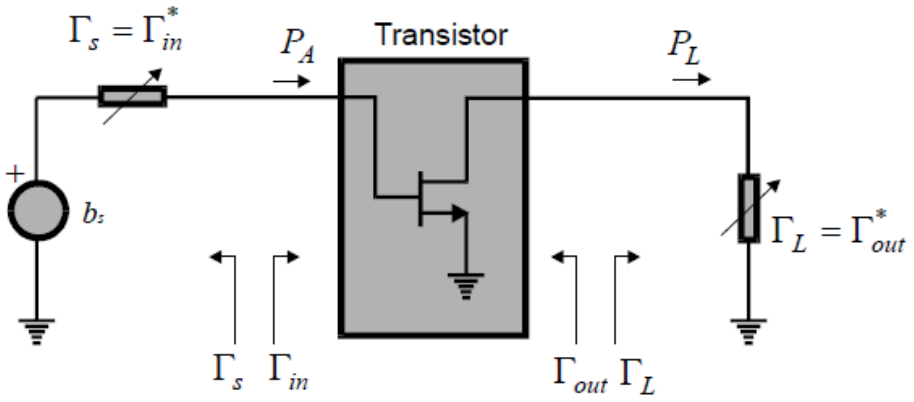

Figure 8.20 Conjugate matching conditions

To solve the simultaneous equations, Γ_L is expressed in terms of Γ_S (from equation (8.61)) and vice versa; which yields:

$$\Gamma_L = \frac{\Gamma_s^* - S_{11}}{\Gamma_s^* S_{22} - D}, \tag{8.63a}$$

$$\Gamma_s = \frac{\Gamma_L^* - S_{22}}{\Gamma_L^* S_{11} - D}. \tag{8.63b}$$

Substituting equation (8.63a) into equation (8.62a) and rearranging results in the quadratic equation in Γ_S (8.64).

$$\Gamma_s^2 - \Gamma_s \frac{B_1}{C_1} + \frac{C_1^*}{C_1} = 0, \tag{8.64}$$

where

$$C_1 = S_{11} - DS_{22}^*, \tag{8.65}$$

$$B_1 = 1 - |S_{22}|^2 + |S_{11}|^2 - |D|^2. \tag{8.66}$$

The solution to this quadratic equation is obtained as:

$$\Gamma_{sM} = \frac{B_1}{2C_1} \pm \frac{1}{2}\sqrt{\left(\frac{B_1}{C_1}\right)^2 - 4\frac{C_1^*}{C_1}} = \frac{C_1^*}{|C_1|}\left[\frac{B_1}{2|C_1|} \pm \sqrt{\frac{B_1^2}{|2C_1|^2} - 1}\right]. \tag{8.67}$$

Here, $B_1/(2|C_1|)$ is a real number and expressed as follows,

$$\frac{B_1}{2|C_1|}=\frac{1+|S_{11}|^2-|S_{22}|^2-|D|^2}{2|S_{11}-S_{22}^*D|}>1, \tag{8.68}$$

Also, $B_1/(2|C_1|)$ is greater than 1 when $k>1$. To prove this, the denominator is expressed as follows:

$$|S_{11}-S_{22}^*D|^2=|S_{12}S_{21}|^2+\left(1-|S_{22}|^2\right)\left(|S_{11}|^2-|D|^2\right), \tag{8.69}$$

Squaring right hand side of equation (8.68) and substituting equation (8.69) gives

$$\left(1+|S_{11}|^2-|S_{22}|^2-|D|^2\right)^2>4|S_{12}S_{21}|^2+4\left(1-|S_{22}|^2\right)\left(|S_{11}|^2-|D|^2\right), \tag{8.70}$$

This can be simplified into,

$$\left[\left(1-|S_{22}|^2\right)+\left(|S_{11}|^2-|D|^2\right)\right]^2-4\left(1-|S_{22}|^2\right)\left(|S_{11}|^2-|D|^2\right)>4|S_{12}S_{21}|^2, \tag{8.71}$$

Making use of the identity $(a+b)^2-4ab=(a-b)^2$ and rearranging the above equation, yields,

$$\left(1-|S_{11}|^2-|S_{22}|^2+|D|^2\right)^2>4|S_{12}S_{21}|^2. \tag{8.72}$$

Thus, $B_1/(2|C_1|)$ is greater than 1 when $k>1$.

This implies that when the transistor is stable, i.e., $k>1$, conjugate matching is always possible. However, the root of equation (8.67) must be chosen such that $|\Gamma_S|\le 1$. Since the magnitude of $(C_1)^*/|C_1|$ outside the bracket [ ] in equation (8.67) is 1, the terms in the bracket [ ] must therefore be less than 1. The terms in the bracket [ ] can be considered in the form $x-\sqrt{x^2-1}$ and $x+\sqrt{x^2-1}$. The term $x+\sqrt{x^2-1}$ becomes greater than 1 for $x\ge 1$, and Γ_{SM} cannot be implemented using passive device. Also matching becomes impossible. Therefore, the applicable solution to equation (8.67) that must be selected is the difference term which is expressed as in (8.73).

$$\Gamma_{sM}=\frac{C_1^*}{|C_1|}\left[\frac{B_1}{2|C_1|}-\sqrt{\frac{B_1^2}{|2C_1|^2}-1}\right]. \tag{8.73}$$

The solution for the output reflection coefficient is also determined using the same approach as above and is given as:

$$\Gamma_{LM}=\frac{C_2^*}{|C_2|}\left[\frac{B_2}{2|C_2|}-\sqrt{\frac{B_2^2}{|2C_2|^2}-1}\right], \tag{8.74}$$

where

$$C_2 = S_{22} - DS_{11}^*, \tag{8.75}$$

$$B_2 = 1 - |S_{11}|^2 + |S_{22}|^2 - |D|^2. \tag{8.76}$$

When k<1, the magnitude of Γ_{SM} and Γ_{LM} is 1 and the source and load impedances become pure imaginary (i.e. inductor or capacitor) and real power is not delivered. That is, when k<1, conjugate matching by equations (8.73) and (8.74) is not possible.

The maximum gain is obtained by substituting the transducer power gain into equations (8.73) and (8.74), but this calculation is a fairly complicated process, and reference [1] can be consulted for details. The gain thus obtained is known as the Maximum Available Gain (MAG), G_{max} which is expressed as follows:

$$MAG = G_{\max} = \left|\frac{S_{21}}{S_{12}}\right|\left(k - \sqrt{k^2 - 1}\right). \tag{8.77}$$

In the case of instability, k<1, meaningful gain can be derived up to the boundary of the stability condition. Thus, substituting k=1 into equation (8.77), the maximum meaningful gain is derived while maintaining stability. This is also known as Maximum Stable Gain (MSG) and is expressed as follows:

$$MSG = \left|\frac{S_{21}}{S_{12}}\right|. \tag{8.78}$$

■ Example 8.3

Use the results of the previous simulation in Example 8.2 and plot **MSG**, **MAG**, and $|S_{21}|^2$ for FHX35LG/LP in the 1~20 GHz band. Find also the conjugate matching points at 12 GHz. .

Solution

Add the following equations in the Display window to obtain **MSG** and **MAG**.

Eqn MaxG=max_gain(S)

Figure 8E.6 Equation for MSG and MAG

The **max_gain(S)** function returns MSG for **k**<1 and returns **MAG** for k>1. Using the values of ***k*** which depends on frequency, it is possible to know whether **max_gain()** represents **MAG** or **MSG**. Thus, by simultaneously plotting **k** values together with the function, the obtained **max_gain** values can be distinguished.

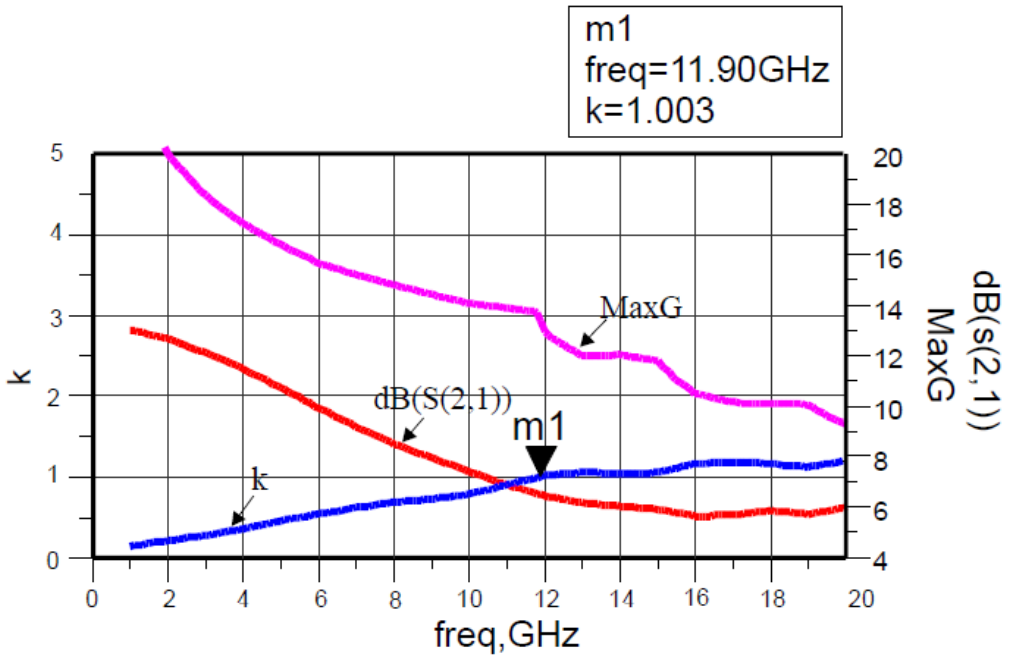

Figure 8E.7 Graph of Max_gain and $|S_{21}|^2$ with respect to frequency

As can be seen from the graph, above the 11.87 GHz, the **max_gain** plot represents **MAG** while it represents **MSG** below this band.

Now we find the input and output conjugate matching points at a frequency of 12 GHz where the active device is stable. ADS functions **sm_gamma1(S)** and **sm_gamma2(S)** are used to find the conjugate matching points. The function **sm_gamma1(S)** gives the input conjugate matching reflection coefficient as expressed in equation (8.73) while the function **sm_gamma2(S)** gives the output conjugate matching reflection coefficient as expressed in equation (8.74). In addition, this function gives 0 when **k** <1, and gives the correct results only when **k** >1. The function **find_index** is added to find the corresponding index number to the frequency 12 GHz.

```
Eqn  m=find_index(freq, 12G)
Eqn  g1=sm_gamma1(S[m])
Eqn  g2=sm_gamma2(S[m])
```

Figure 8E.8 Equations for obtaining the conjugate matching points

Figure 8E.9 represents the results obtained using the equations.

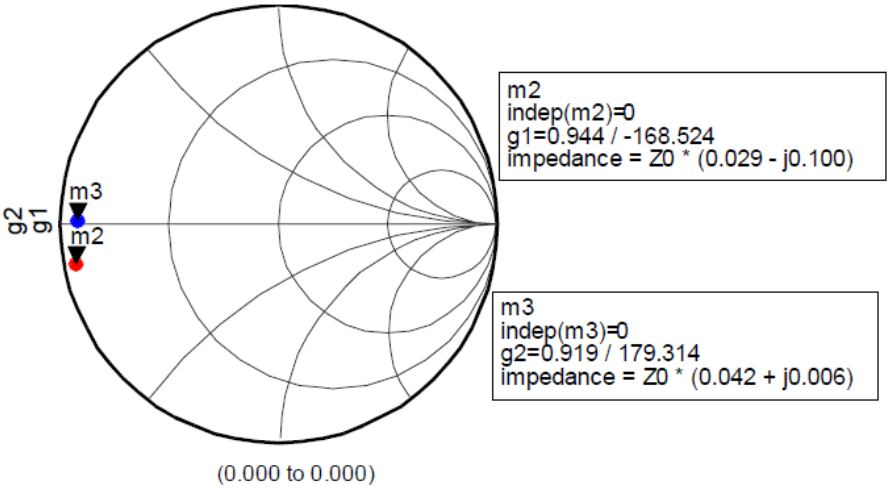

Figure 8E.9 Conjugate matching points at 12 GHz

Therefore, the conjugate matching points at 12 GHz, as can be seen from the above simulation results, are:

$$\Gamma_{sM} = -0.925 - j0.188,$$

$$\Gamma_{LM} = -0.919 + j0.011.$$

■

8.3 GAIN AND NOISE CIRCLES

In general, when source and load reflection coefficients are set by the conjugate matching conditions described previously, maximum gain is obtained; however because other performance must also be considered from design perspective, setting the conjugate matching points can be difficult. When the conjugate matching points cannot be thus set, the gain decreases. Two cases can be considered. That is, the case when the source impedance cannot be selected as the conjugate matching impedance and the case when the load impedance cannot be selected as the conjugate matching impedance. In this case, by considering the design aspects, when the remaining ports meet the conjugate matching conditions, while conjugate matching is not achieved for the selected source or load, it is often necessary to predict the subsequent decrease in gain during the design. In this chapter, we shall examine constant gain circles as well as the circles of reflection coefficient giving the same noise figure, which appeared previously in Chapter 4.

8.3.1 Gain Circles

The equation previously determined for power gain (8.34) can be expressed as follows:

$$G_p = \frac{\left(1-\left|\Gamma_L\right|^2\right)\left|S_{21}\right|^2}{1-\left|S_{11}\right|^2+\left|\Gamma_L\right|^2\left(\left|S_{22}\right|^2-\left|D\right|^2\right)-2\,\mathrm{Re}\left(C_2\Gamma_L\right)}, \tag{8.79}$$

where C_2 is defined as

$$C_2 = S_{22} - DS_{11}^*. \tag{8.80}$$

In addition, for ease of mathematical computation, a normalized gain parameter g_p is defined as follows,

$$g_p = \frac{G_p}{\left|S_{21}\right|^2}. \tag{8.81}$$

The locus of Γ_L giving the same gain when g_p is a constant will satisfy equation (8.79). Therefore equation (8.79) can be rewritten as follows:

$$g_p = \frac{\left(1-\left|\Gamma_L\right|^2\right)}{1-\left|S_{11}\right|^2+\left|\Gamma_L\right|^2\left(\left|S_{22}\right|^2-\left|D\right|^2\right)-2\,\mathrm{Re}\left(C_2\Gamma_L\right)}. \tag{8.82}$$

With the following definitions,

$$D_2 = \left|S_{22}\right|^2 - \left|D\right|^2, \tag{8.83}$$

$$X = \frac{1+g_pD_2}{g_p}. \tag{8.84}$$

equation (8.82) can be rewritten as follows:

$$X^2\left|\Gamma_L\right|^2 - 2X\,\mathrm{Re}\left(C_2\Gamma_L\right)+\left|C_2\right|^2 = X^2B_2+\left|C_2\right|^2, \tag{8.85}$$

Arranging this,

$$\left|X\Gamma_L - C_2^*\right|^2 = X^2 - XB_2 + \left|C_2\right|^2. \tag{8.86}$$

Rearranging equation (8.86), the following equation of a circle can be obtained.

$$\left|\Gamma_L - \frac{C_2^*}{X}\right|^2 = \frac{X^2 - XB_2 + \left|C_2\right|^2}{X^2}. \tag{8.87}$$

Therefore, the center and radius of the circle giving the same power gain as equation (8.87) are as follows:

$$C_p = \frac{C_2^*}{X} = \frac{g_p\left(S_{22}^* - D^* S_{11}\right)}{1 + g_p\left(\left|S_{22}\right|^2 - \left|D\right|^2\right)}, \tag{8.88}$$

$$r_p = \frac{\sqrt{1 - 2k\left|S_{12}S_{21}\right| g_p + \left|S_{12}S_{21}\right|^2 g_p^2}}{\left|1 + g_p\left(\left|S_{22}\right|^2 - \left|D\right|^2\right)\right|}. \tag{8.89}$$

The circle thus obtained is called the power gain circle. In addition, Γ_L is changed to Γ_S and the subscript 1 and 2 are interchanged in equation (8.79) to obtain the following equation for the available power gain:

$$G_A = \frac{\left(1 - \left|\Gamma_s\right|^2\right)\left|S_{21}\right|^2}{1 - \left|S_{22}\right|^2 + \left|\Gamma_s\right|^2\left(\left|S_{11}\right|^2 - \left|D\right|^2\right) - 2\,\mathrm{Re}\left(C_1\Gamma_s\right)}, \tag{8.90}$$

$$C_1 = S_{11} - DS_{22}^*. \tag{8.91}$$

Therefore, to obtain the locus of Γ_S giving the same gain, the following normalized gain is defined.

$$g_A = \frac{G_A}{\left|S_{21}\right|^2} \tag{8.92}$$

Interchanging the subscripts 1 and 2 in equations (8.88) and (8.89) will yield the radius and center for the available gain circle. Thus

$$C_A = \frac{g_a\left(S_{11}^* - D^* S_{22}\right)}{1 + g_a\left(\left|S_{11}\right|^2 - \left|D\right|^2\right)}, \tag{8.93}$$

$$r_a = \frac{\sqrt{1 - 2k\left|S_{12}S_{21}\right| g_p + \left|S_{12}S_{21}\right|^2 g_a^2}}{\left|1 + g_a\left(\left|S_{11}\right|^2 - \left|D\right|^2\right)\right|}. \tag{8.94}$$

The circles thus obtained are called the available gain circles which give the same available power gain.

8.3.2 Noise Circles

The noise figure obtained in Chapter 4 in terms of the noise parameters depends only on the the source reflection coefficient Γ_S which is expressed as follows.

$$F = F_{\mathrm{m}} + 4r_n \frac{\left|\Gamma_s - \Gamma_m\right|^2}{\left|1+\Gamma_m\right|^2\left(1-\left|\Gamma_s\right|^2\right)}. \tag{8.95}$$

To obtain the locus of Γ_S giving the same noise figure, a new noise figure is defined for computational simplicity as

$$N_i = \frac{F_i - F_m}{4r_n}\left|1+\Gamma_m\right|^2, \tag{8.96}$$

The noise figure equation can then be written as follows:

$$N_i = \frac{\left|\Gamma_s - \Gamma_m\right|}{1-\left|\Gamma_s\right|^2}. \tag{8.97}$$

Expanding, this can be written as:

$$\left|\Gamma_s - \Gamma_m\right|^2 = \left|\Gamma_s\right|^2 + \left|\Gamma_m\right|^2 - 2\,\mathrm{Re}\left(\Gamma_s\Gamma_m^*\right) = N_i - N_i\left|\Gamma_s\right|^2, \tag{8.98}$$

which is rearranged as follows:

$$\left|\Gamma_s\right|^2\left(1+N_i\right) + \left|\Gamma_m\right|^2 - 2\,\mathrm{Re}\left(\Gamma_s\Gamma_m^*\right) = N_i, \tag{8.99}$$

Multiplying both sides of (8.99) by $(1+N_i)$ results in the following:

$$\left|\Gamma_s\right|^2\left(1+N_i\right)^2 + \left|\Gamma_m\right|^2 - 2\left(1+N_i\right)\mathrm{Re}\left(\Gamma_s\Gamma_m^*\right) = N_i^2 + N_i\left(1-\left|\Gamma_m\right|^2\right). \tag{8.100}$$

Thus, the locus of Γ_S giving the same N_i is as given by the circle equation below:

$$\left|\Gamma_s - \frac{\Gamma_m}{1+N_i}\right|^2 = \frac{N_i^2 + N_i\left(1-\left|\Gamma_m\right|^2\right)}{\left(1+N_i\right)^2}. \tag{8.101}$$

Therefore, the radius and center of this circle are expressed as follows:

$$C_F = \frac{\Gamma_m}{1+N_i}. \tag{8.102a}$$

$$r_F = \frac{\sqrt{N_i^2 + N_i\left(1-\left|\Gamma_m\right|^2\right)}}{1+N_i} \tag{8.102b}$$

■ Example 8.4

Using the FHX35LG/LP, draw the noise circles and the available power gain circles at 12 GHz.

Solution

To calculate the noise parameters, open the S-parameter controller and check Calculate Noise and then specify the Noise input/output port. Simulate and then enter the following equations in Fig. 8E.11 in the Display window to draw the circles.

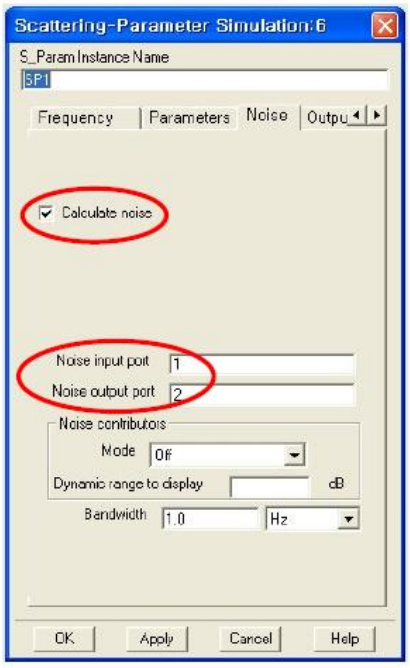

Figure 8E.10 Setting the calculate noise of the S-parameter controller

```
Eqn  ga1=ga_circle(S[m])
Eqn  ns1=ns_circle({0,1,2,3}+NFmin[m], NFmin[m], Sopt[m], Rn[m]/50, 51)
```

Figure 8E.11 Equations for drawing the locus of available power gain circle and noise circles.

The function **ns_circle()** is used for drawing the noise circles giving by equation (8.102) while the function **ga_circle()** is used for drawing available power gain circles given by equations (8.93) and (8.94). The function **ga_circle()** draws the available power gain circles lower than the conjugate matched gain or **MAG** by {1,2,3} dB as the default. The circles plotted by equation in Fig. 8E.11 are shown on the Smith chart. The maximum point of the available power gain circle in Fig. 8E.12 is the conjugate matching point of the source reflection coefficient.

In addition, the variable of the function **ns_circle()**, **{0,1,2,3}+NF$_{min}$** represents noise figure circles {1,2,3} dB lower than the minimum noise figure; and the corresponding noise parameters **NFmin[m]**, **Sopt[m]** and **Rn[m]/50** are required. It must be noted that the function **ns_circle()** uses the normalized noise resistance by 50 ohm. The 51 represents the number of sample points used for drawing the circle.

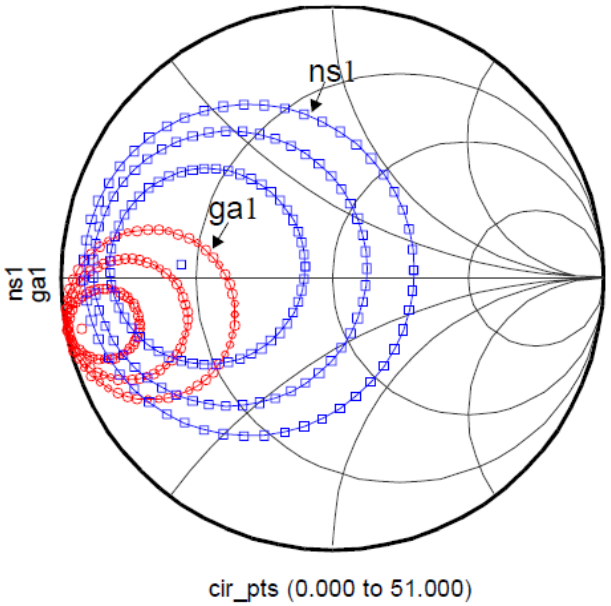

Figure 8E.12 Noise and available power gain circles

■

8.4 SUMMARY

8.4.1 Summary of Gains

Transducer power gain G_T is the normal power gain which is used during amplifier measurement, and is defined as the power delivered to the load from the available power of the source. In the case of the measurement for a 50 ohm source and load, that is $\Gamma_S=\Gamma_L=0$, the transducer power gain results in $|S_{21}|^2$; this is the transducer power gain for 50 ohm.

The available power gain is the gain for the source reflection coefficient when the output is matched. This represents the degradation in gain due to the fixed source reflection coefficient and is used to evaluate the gain decrease during design. Similarly, the power gain is the gain for the selected load when the input side is always conjugate matched, and represents the gain degradation for selected load reflection coefficient.

Next, the maximum gain is achieved when both input and output of the active device are conjugate matched. The maximum available power gain, MAG can be obtained if the device is stable; and when it is unstable, the maximum stable gain, MSG can be obtained at the stability boundary k=1. As this calculation is complex, intuitive evaluation of the result is also difficult and

so unilateral approximation is applied in which case the maximum unilateral gain is obtained. This also shows the extent of the improvement on the transducer power gain $|S_{21}|^2$, resulting from conjugate matching. Also the passivity or activity of a device, which is whether a device can amplify or not, can be found using the Mason's gain, which is the gain obtained after the removal of feedback from output to input.

Table 8.1 Gain formulas given in terms of S-parameters

Gain	Formula
Tranducer power gain in 50-ohm	$G_T = \|S_{21}\|^2$
Tranducer power Gain	$G_T = \frac{(1-\|\Gamma_L\|^2)\|S_{21}\|^2(1-\|\Gamma_S\|^2)}{\|(1-S_{22}\Gamma_L)(1-S_{11}\Gamma_S)-S_{12}S_{21}\Gamma_L\Gamma_S\|^2}$
Power Gain	$G_P = \frac{(1-\|\Gamma_L\|^2)\|S_{21}\|^2}{\|1-S_{22}\Gamma_L\|^2(1-\|\Gamma_{in}\|^2)}$
Available power Gain	$G_A = \frac{P_{Ao}}{P_{Ai}} = \frac{(1-\|\Gamma_S\|^2)\|S_{21}\|^2}{\|1-S_{11}\Gamma_S\|^2(1-\|\Gamma_{out}\|^2)}$
Mason's unilateral Gain	$U = \frac{\|S_{21}/S_{12}-1\|^2}{2k\|S_{21}/S_{12}\|-2\,\mathrm{Re}(S_{21}/S_{12})}$
Maximum Unilateral Power Gain	$G_{TU\max} = \frac{\|S_{21}\|^2}{(1-S_{22}{}^2)(1-S_{11}{}^2)}$
Maximum Stable Gain	$G_{ms} = \left\|\frac{S_{21}}{S_{12}}\right\|$
Maximum Available Gain	$G_{ma} = \left\|\frac{S_{21}}{S_{12}}\right\|(k-\sqrt{k^2-1})$

$$\text{Stability Factor, } k = \frac{1-|S_{11}|^2-|S_{22}|^2-|D|^2}{2|S_{12}S_{21}|}.$$

8.4.2 Summary of Circles

The center and radius derived previously for drawing circles in the Smith chart are summarized in Table 8.2. The available power gain circles are the loci of the source reflection coefficient Γ_S

yielding the same available gain decrease from MAG. Note that the load is assumed to be conjugate matched to the output reflection coefficient given by Γ_S. Conversely, the power gain circles are the loci of the load reflection coefficient Γ_L giving the same gain decrease from MAG. In plotting the circles, it is assumed that the source reflection coefficient is conjugate matched to the input reflection coefficient given by Γ_L. This shows gain degradation for a selected load reflection coefficient. Together with the available power gain circles, these are commonly used to evaluate gain degradation from MAG for the selected load or source reflection coefficients during the design. Noise circles are used to evaluate the consequent degradation of the noise figure when the source reflection coefficient is not selected for the minimum noise figure; and they are commonly used together with the available gain circles mentioned previously in low noise amplifier design.

The stability circles help us to know whether negative resistance appear at the input or output for the selected load or source reflection coefficients and to know whether there is the possibility of oscillation or not. Accordingly, we are able to know the region of stability where the load or source reflection coefficients do not induce negative resistance at the input or output. Source stability circles determine whether the selected source reflection coefficient is in the region of stability or not while the load stability circles determine whether the selected load reflection coefficient is in the region of stability or not.

Table 8.2 Formula of the various circles given in S-parameters

Circles	Center	Radius
Available Gain	$C_a = \dfrac{g_a(S_{11}^* - D^* S_{22})}{1+g_a(\lvert S_{11}\rvert^2 - \lvert D\rvert^2)}$	$r_a = \dfrac{\sqrt{1-2k\lvert S_{12}S_{21}\rvert g_a + \lvert S_{12}S_{21}\rvert^2 g_a^2}}{\lvert 1+g_a(\lvert S_{11}\rvert^2 - \lvert D\rvert^2)\rvert}$
Power Gain	$C_p = \dfrac{g_p(S_{22}^* - D^* S_{11})}{1+g_p(\lvert S_{22}\rvert^2 - \lvert D\rvert^2)}$	$r_p = \dfrac{\sqrt{1-2k\lvert S_{12}S_{21}\rvert g_p + \lvert S_{12}S_{21}\rvert^2 g_p^2}}{\lvert 1+g_p(\lvert S_{22}\rvert^2 - \lvert D\rvert^2)\rvert}$
Noise Mismatch	$C_F = \dfrac{\Gamma_m}{1+N_i}$	$r_F = \dfrac{\sqrt{N_i^2 + N_i(1-\lvert\Gamma_m\rvert^2)}}{(1+N_i)}$
Source Stability	$C_s = \dfrac{S_{11}^* - D^* S_{22}}{\lvert S_{11}\rvert^2 - \lvert D\rvert^2}$	$r_s = \dfrac{\lvert S_{12}S_{21}\rvert}{\lvert \lvert S_{11}\rvert^2 - \lvert D\rvert^2\rvert}$
Load Stability	$C_L = \dfrac{S_{22}^* - D^* S_{11}}{\lvert S_{22}\rvert^2 - \lvert D\rvert^2}$	$r_L = \dfrac{\lvert S_{12}S_{21}\rvert}{\lvert \lvert S_{22}\rvert^2 - \lvert D\rvert^2\rvert}$

Normalized power gain, $g_p = \dfrac{G_p}{\lvert S_{21}\rvert^2}$,

Normalized availale power gain, $g_A = \dfrac{G_A}{\lvert S_{21}\rvert^2}$,

Normalized noise figure, $N_i = \dfrac{F_i - F_m}{4r_n}\lvert 1+\Gamma_m\rvert^2$.

8.5 LOW NOISE AMPLIFIER DESIGN EXAMPLE

Low noise amplifier is an amplifier having a low noise figure, and usually located at the front-end of a receiver. According to the Frii's formula, the overall noise figure depends not only on the noise figure of the front-end amplifier, but is also related to the noise figure of subsequent stages. Thus, the overall noise figure depends on both the noise figure and gain of the low noise amplifier. In this sense, the design of the low noise amplifier can be viewed as a trade-off design between noise figure and gain. The design involves a process of appropriate active device selection, the selection of optimal source and load impedances, matching circuit design, addition of DC bias circuit, and investigation of stability. The selected active device is sometimes unstable at the design frequency. In such case, stabilization is achieved through feedback or adding small losses to the active device. Refer to [1] for details of this method. In addition, the last step of stability check needs to be given considerable attention since there is often the possibility of oscillation in the designed low noise amplifier at frequencies other than the design frequency. This chapter explains low noise amplifier design using ADS based on the theories previously discussed.

8.5.1 Design Goal

This section is based on the theories previously discussed in this chapter. Since the goal is to learn about simple low noise amplifier design, the design specifications shown in Table 8.3 were selected for the low noise amplifier operating in X-band (8-12 GHz frequency band, say). The appropriate active device must then be selected for the given design specifications. Firstly, an active device with minimum noise figure, F_{min} lower than the design goal noise figure at the design frequency is selected; the maximum gain, MAG of the selected active device must be greater than the desired gain. An appropriate active device satisfying the design goal may not be available. In that case, the gain can be increased to meet the design goal by cascading a number of stages. Therefore, it should be noted that the key parameter is the selection of the noise figure. ATF-36077, the S-parameter of which is provided in ADS, is selected to meet the required 1 stage gain and noise figure of the active device.

Table 8.3 Low noise amplifier design specification example

NO.	Spec Item	Value
1	Frequency Range	9.7 ~ 10.3 GHz
2	DC Supply Voltage	3.3 V
3	DC current Consumption	< 30 mA
4	Gain	> 10 dB
5	Noise Figure	< 1.5 dB

8.5.2 Active Device Model Investigation

The models used in the low noise amplifier design can be categorized as large-signal model and S-parameter data model measured at the given DC voltage. The S-parameters generated using the large-signal model of a packaged active device at a given DC voltage does not generally reflect the measured S-parameters with the desired accuracy, due to the inaccuracy of the large signal model caused by the complexity of the equivalent circuit including parasitic elements from the package

assembly. Although the large-signal model of a chip type active device has some degree of accuracy, the large signal model of a packaged active device generally does not show sufficient accuracy. Thus, the design is generally carried out using the measured S-parameter in the design of a low noise amplifier using packaged device. These data-models are sometimes already available in the ADS library, otherwise the user needs to construct the data model by directly entering the given measurement results.

Figure 8.21 shows a small signal data-model of the ATF-36077 provided in ADS. This model has S-parameter values for 0.5 GHz to 18 GHz at $\mathbf{V_{ds}}$=1.5 V and $\mathbf{I_d}$=20 mA; no separate DC bias circuit is required to operate this device and it can be simulated just from RF signal alone.

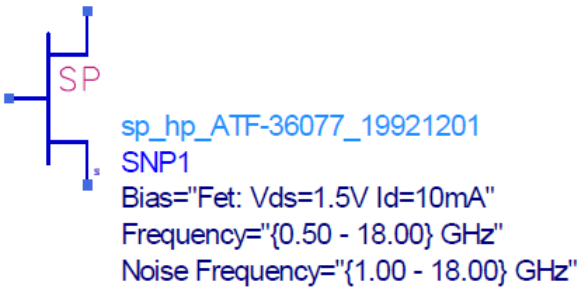

Figure 8.21 Small-signal data model of the ATF-36077

To design using the large-signal model, DC voltage is applied and the S-parameters are extracted at the applied DC voltage as previously described in chapter seven.

8.5.3 Stability

Figure 8.22 is an S-parameter simulation circuit set up for investigating the stability and maximum gain (**MSG** or **MAG**) as well as the minimum noise figure with respect to frequency for the selected active device. This investigation can be accomplished in the Display window using the built-in measurement expressions for the simulated S-parameters; however, this measurement expression is also available in the Schematic window as shown in Fig. 8.22.

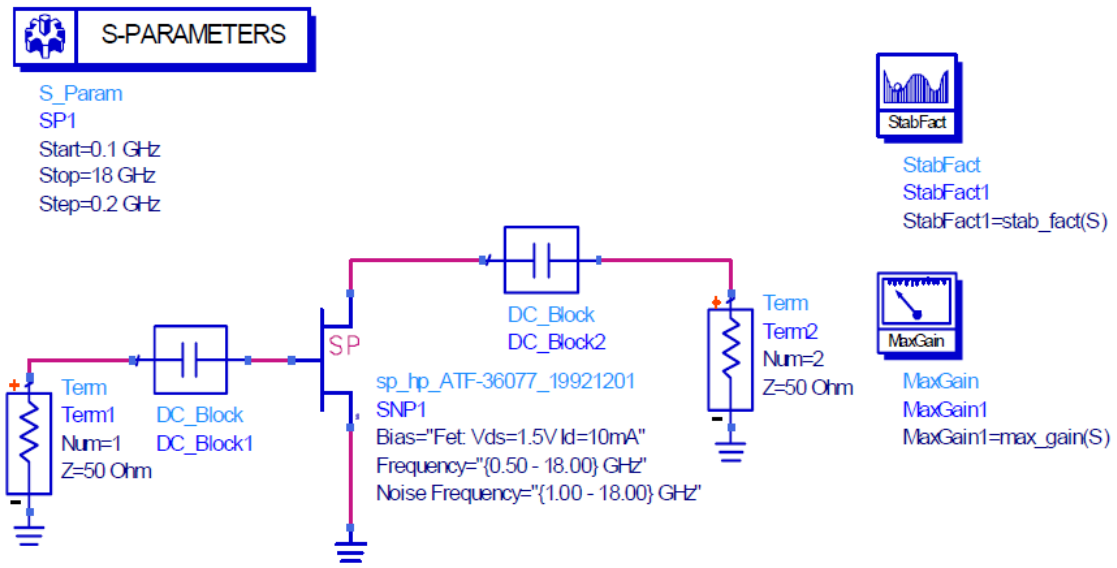

Figure 8.22 Investigation of the and gain stability of the ATF-36077

The simulated results are shown in Fig. 8.23. As can be seen from the results, **k** is less than 1 below 10 GHz, and greater than 1 above 10 GHz. As described in the previous section, the maximum gain can be calculated using previously presented equations of **MSG** in which **k** is less than 1 and of **MAG** in which **k** is greater than 1. However this is done automatically when **MaxGain** measurement expression in ADS is used. It is worth noting in Fig. 8.23(b) that, $\mathbf{NF_{min}}$ is constant at 0.3 dB below 6 GHz. This is not a simulation error; in the author's opinion, the noise figure below 0.3 dB could not be accurately measured which is considered to be due to the loss of accuracy in the entered data.

Therefore, stabilization is necessary to have **k** greater than 1 at 10 GHz. Considering the design goal of bandwidth, **k** should be greater than 1 from 9.7 GHz for safer design.

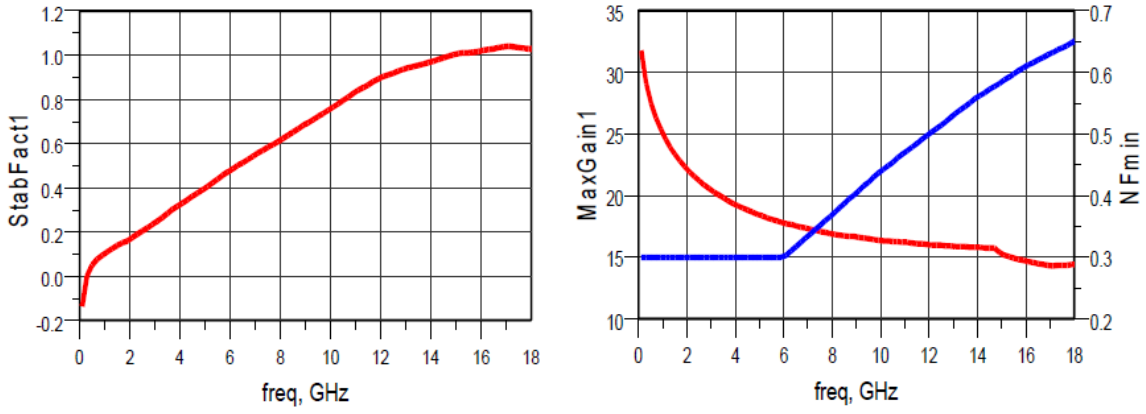

Figure 8.23 (a) ***k*** and (b) maximum gain and NF_{min} with respect to frequency

One way of improving the stability is shown in Fig. 8.24; an inductor $\mathbf{L_e}$ is connected to the source terminal of the active device. In this method, the inductor added to the source terminal is

used to vary the S-parameters which results in the change of the stability factor. Figure 8.24 is a circuit set up in which the inductance is varied from 0 to 0.3 nH at a fixed frequency of 10 GHz to evaluate the variation in **k**.

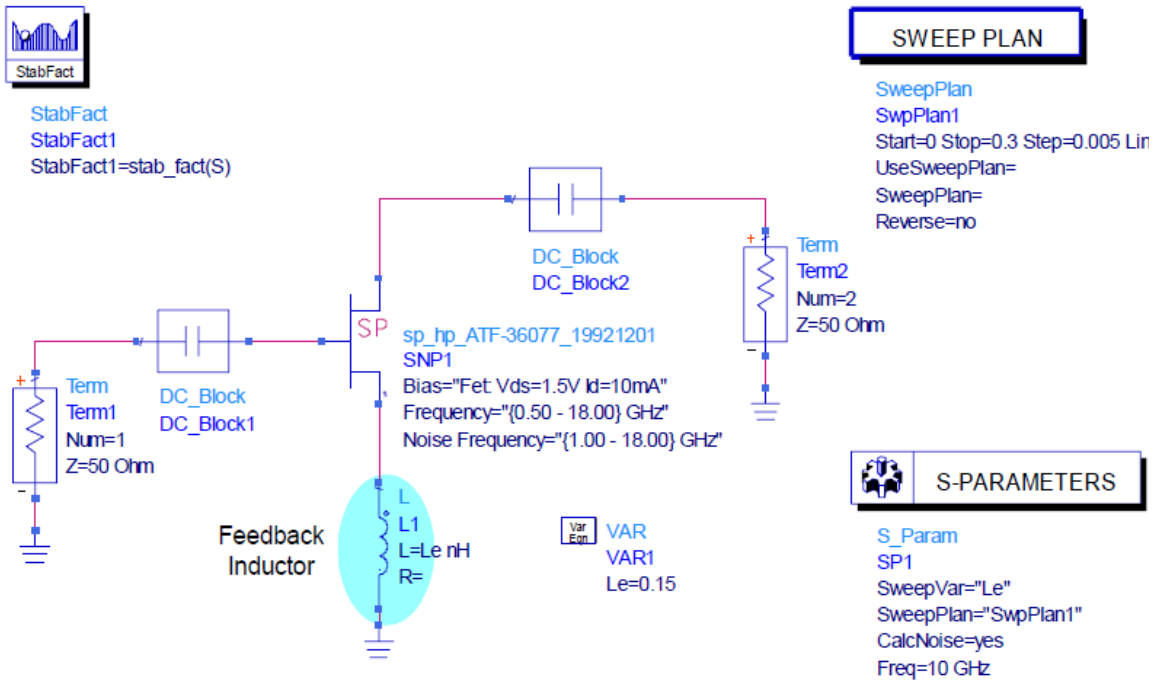

Figure 8.24 Schematic for evaluating the variation of k due to the series feedback inductor.

The results are shown in Fig. 8.25. From the results of Fig. 8.25(a), **k** has a maximum value of 1.031 at 10 GHz when L_e is approximately 0.05 nH and stability is thus achieved. Therefore, L_e is set to 0.05 nH and **k** is plotted with respect to frequency as shown in Fig. 8.25(b), which shows **k** greater than 1 at the desired frequency.

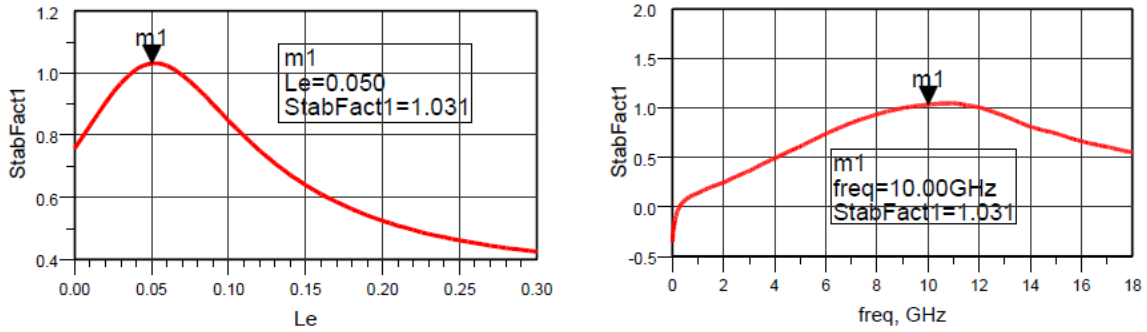

Figure 8.25 (a) Stability factor with respect to the value of Le at 10 GHz and (b) the frequency response of **k** for L_e**=0.05 nH**.

The improvement in the **k** value that was achieved by the addition of L_e satisfies **k** >1, however, the bandwidth is narrow and the **k** value is too close to 1. There are several other ways to improve

the stability of the circuit beyond this value; addition of a load resistor is one of the methods commonly used [1, p228]. The method of improving **k** by the addition of parallel resistors to the output terminal is selected in this book. Figure 8.26 is a circuit in which a 35 ohm resistor (for improving the value of **k**) is connected in series to a 100 nF capacitor which provides RF ground. The microstrip lines represent connecting conductor patterns for mounting the chip resistor and capacitor. This circuit is connected to the drain terminal of the transistor. The reason for this connection is to minimize the impact on the noise factor of the circuit. In addition, this two-port circuit is configured as a subcircuit. That is, by converting functional circuit parts into subcircuits as shown in Fig. 8.26, complex schematics can be avoided during the design of complex wired circuits; allowing the amplifier circuit to be represented in a simple schematic.

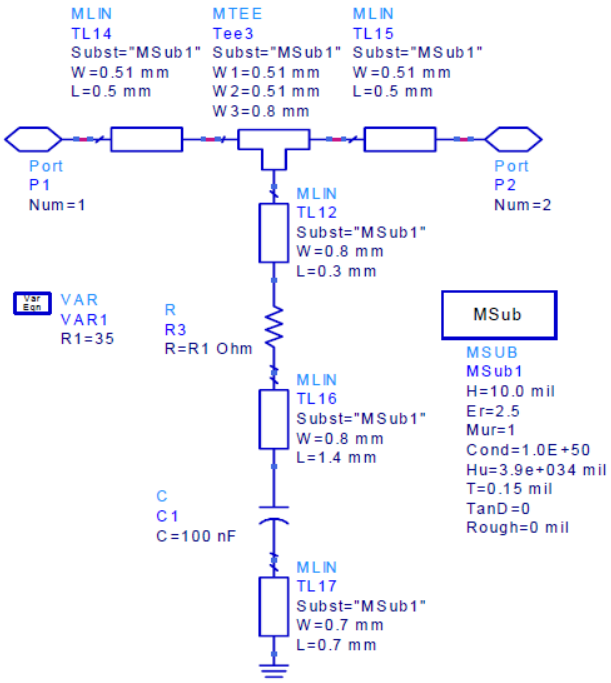

Figure 8.26 Resistance circuit added for increasing **k**; Subcircuit (**R_stab**)

Parameter sweep is used to vary the value of the resistance from 0 to 50 ohm to investigate the variation in **k** after the addition of the **R_stab subcircuit** to the circuit of Fig. 8.24. Figure 8.27(a) shows the result for **k**. The stability factor is plotted for a range of 0-18 GHz frequency in Fig. 8.27(b) for the value of 35 ohm **R_stab subcircuit**. The decreased gain due to the resistance added for stabilization is slightly compensated by modifying L_e=0.04 nH. As a result of the addition of the subcircuit, the stability factor is found to be greater than 1 for a wider frequency range.

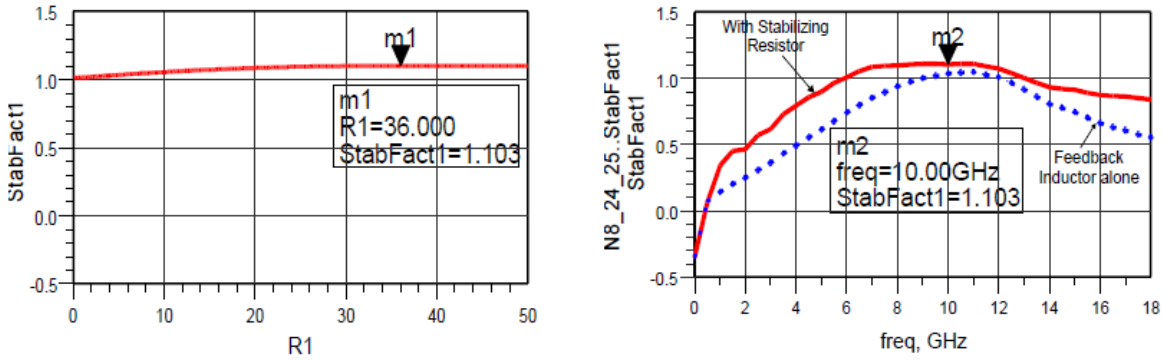

Figure 8.27 Frequency-dependent variation of **k** due to the added **R_stab** (a) the stability factor with respect to resistance (at 10 GHz fixed frequency), (b) frequency-dependent variation of ***k*** when the resistance is 35 ohm.

8.5.4 Selection of Source and Load Impedances

In this section, we shall examine the variation of gain and noise factor with respect to the source and load reflection coefficients; we shall also examine the selection of source and load reflection coefficients to match the design goals. Figure 8.28 is a circuit set up, in which the feedback inductor $\mathbf{L_e}$ and **R_stab** subcircuit are added to the active device to examine the variation of the available power gain and the noise circles at 10 GHz with respect to the source reflection coefficient. This can be carried out in the Display window; however, here we use the measurement expressions in the Schematic window. In Fig. 8.28, three gain circles whose gain reduces by 1 dB step from the maximum available gain (**MAG**) value; and three noise circles whose noise figure increases by 0.2 dB step from the minimum noise figure $\mathbf{NF_{min}}$ value were selected to illustrate the available gain and noise circles respectively.

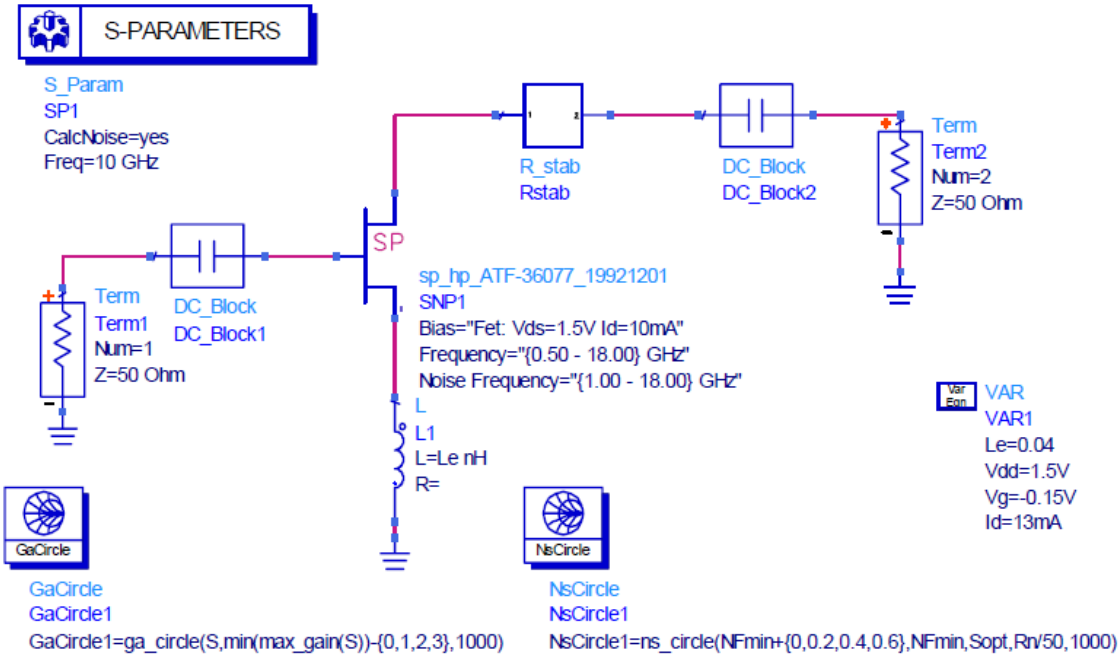

Figure 8.28 Circuit set up for measuring available power gain and noise circles

The available gain and noise circles for such simulation are as shown in Fig. 8.29.

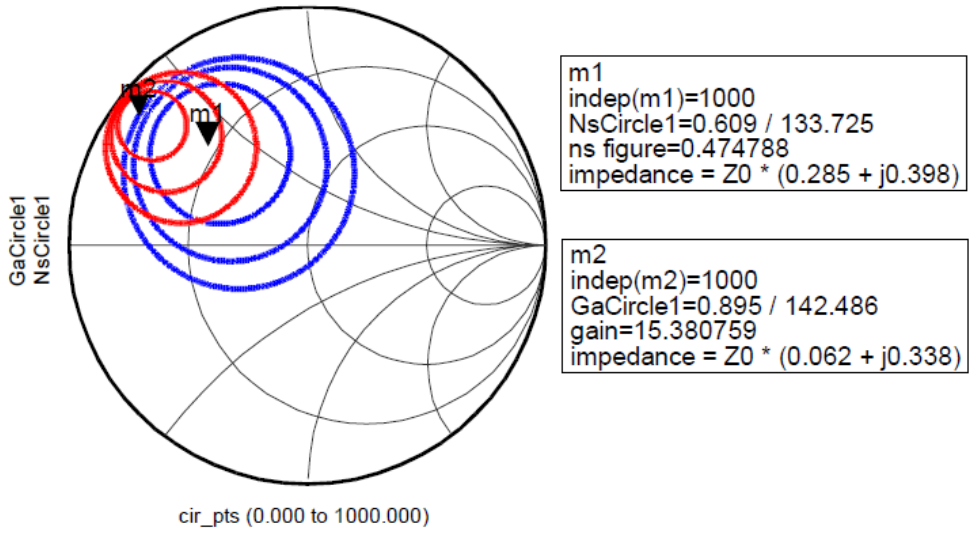

Figure 8.29 Available power gain and noise circles

Marker m1 represents the minimum value of the noise circle (0.47dB) while **marker m2** represents the maximum value of the available gain circles (15.38 dB). The gain

and noise figure performance thus differ depending on the choice of source reflection coefficient. The source and load impedances must therefore be properly chosen in accordance with the design goal. Considering the given specifications of 10 dB gain and 1.5 dB noise figure, the source reflection coefficient Γ_S was selected as **marker m1** having minimum noise figure of 0.47 dB. From the selection results of Fig. 8.29, noise figure of 0.5 dB and gain of 13 dB or more can be expected.

The source reflection coefficient thus selected is $\Gamma_S = m1 = 0.609 \angle 133.725°$; for which the corresponding conjugate matching load reflection coefficient is given by:

$$\Gamma_L = \left(S_{22} + \frac{S_{12} S_{21} \Gamma_s}{1 - S_{11} \Gamma_s} \right)^* = 0.548 \angle -159.05,$$

which when converted to impedance are given by the following source and load impedances:

$$Z_{source} = \left(Z_{in} \right)^* = 50 * \left(0.285 + j0.398 \right),$$

$$Z_{load} = \left(Z_{out} \right)^* = 50 * \left(0.301 - j0.169 \right).$$

The circuit of Fig. 8.30 is set up to confirm the obtained results by measuring the gain and noise figure at the design frequency. It must be noted that, since the source and load port impedances have the impedance values obtained in the above result, by using these impedances, it can be determined whether the expected gain and noise figure could be achieved.

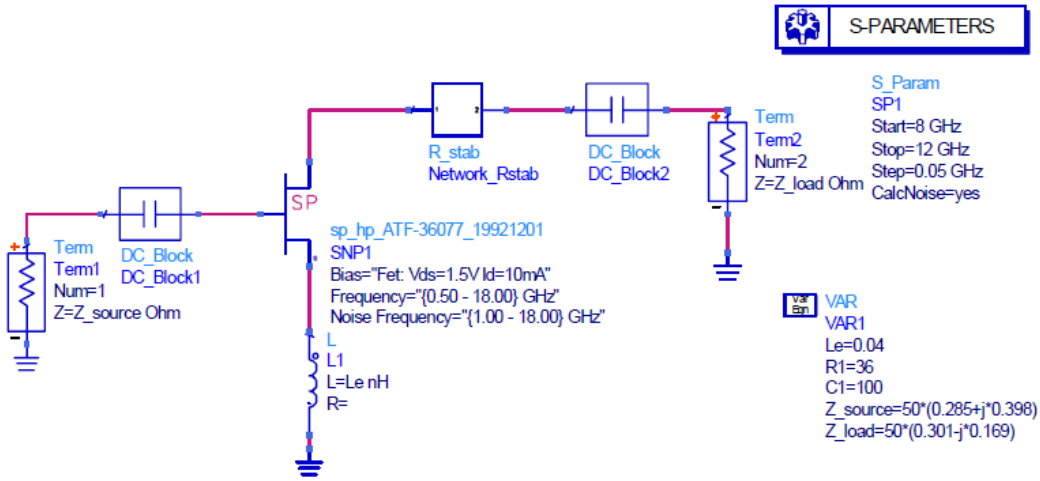

Figure 8.30 Schematic for confirming the source and load impedances

The result of Fig. 8.31 is obtained from the simulation of the above circuit. As expected, the gain is found to be more than 13 dB and the noise figure below 1.5 dB in the desired frequency band. Therefore, this set of source and load impedances is found to be the appropriate choice for the desired low noise amplifier.

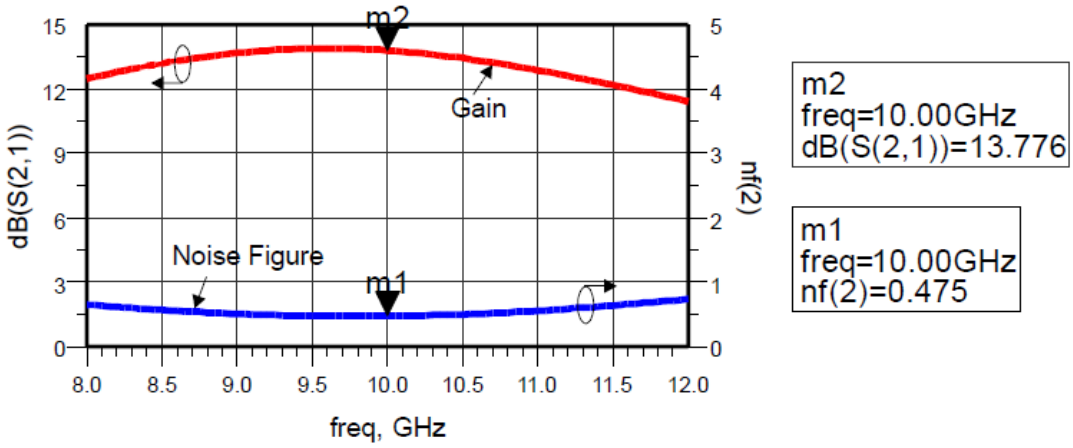

Figure 8.31 Gain and noise figure results for the selected source and load impedances

8.5.5 Matching Circuit Design

The desired gain and noise figure that can be obtained when the previously selected source and load impedances are connected to the active device has been confirmed. However, actual sources and loads are typically 50 Ω, and matching circuits are needed to convert the 50 Ω source and load impedances to the previously selected impedances required by the low noise amplifier. These matching circuits can be designed using the theories previously explained in chapter six, for this purpose however, optimization technique available in ADS will be used for the matching. In addition, transmission lines and distributed circuits are generally required at a frequency of 10 GHz; and when microstrip line are used, the matching is limited by discontinuity effects making it difficult to determine whether the matching actually works or not. Therefore, in this chapter we first use lumped-elements to design the matching circuit and then determine the matching circuit with the obtained results using transmission lines.

8.5.5.1 Lumped Element Matching Circuits

Matching at 10 GHz using Optimization technique in ADS is shown in Fig. 8.32. It must be noted that, the impedance of port 1 is 50 ohm while that of port 2 is the complex conjugate of the previously determined source impedance. Therefore, if the matching is to be achieved for maximum power transfer under this condition, since the impedance looking into port 1 from port 2 must be the complex conjugate of port 2 impedance, the impedance of port 2 must be the desired source impedance. Therefore, the 50 ohm port and matching circuit are implemented with the desired source impedance value.

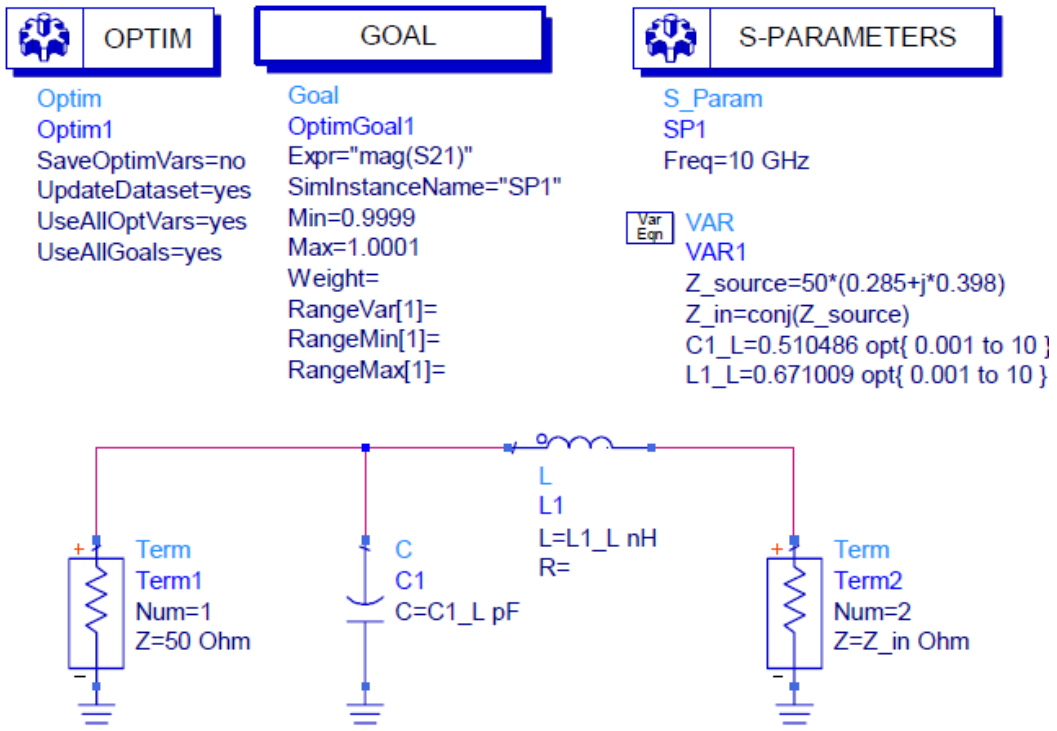

Figure 8.32 Lumped elements input matching circuit set up

Under this condition, the goal is to change the values of **C** and **L** until maximum power is delivered, which is to set the magnitude of S_{21} to 1. After simulation, the magnitude of S_{21} is found to be closest to 1 when **C** is 0.510 pF and **L** is 0.671 nH.

Figure 8.33 is the S-Parameter Simulation results on a polar plot, after the optimization result of the circuit in Fig. 8.32 is updated in the variables. It can be seen that the magnitude of S_{21} is 1 while those of S_{11} and S_{22} are 0 indicating impedance matching. As the circuit is matched, maximum power is transferred and as such, $|S_{21}|^2=1$. Since this is a lossless matching circuit, $|S_{11}|^2+|S_{21}|^2=1$, from which it can be inferred that $S_{11}=0$. In addition, as this is a passive circuit $S_{21}= S_{12}$, and invoking the lossless condition, it can also be seen that $S_{22}=0$.

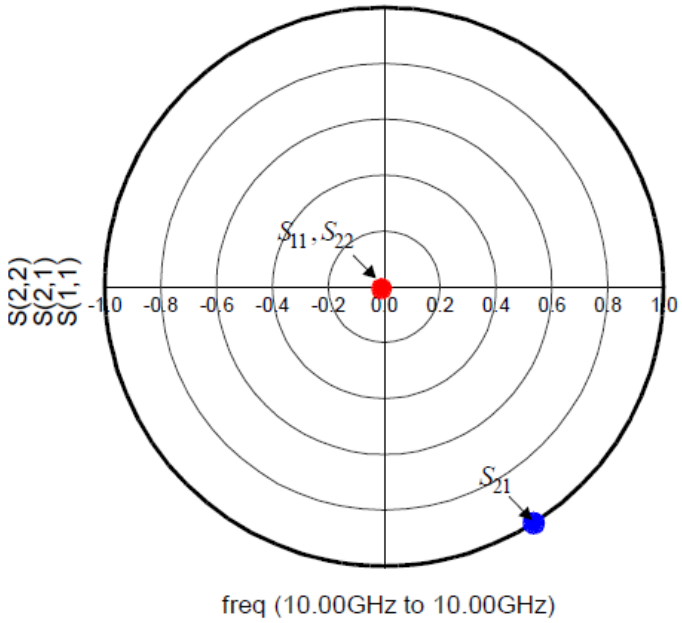

Figure 8.33 Simulation results of the input matching circuit (frequency 10 GHz)

The output matching circuit at 10 GHz (using the same method) is set up as shown in Fig. 8.34 and the obtained results after optimization are 0.478 pF for ***C*** and 0.231 nH for ***L***. To determine whether matching has been achieved, the simulation result is shown in polar plot in Fig. 8.35. From this result, the magnitude of S_{21} is 1 while those of S_{11} and S_{22} are 0, indicating impedance matching.

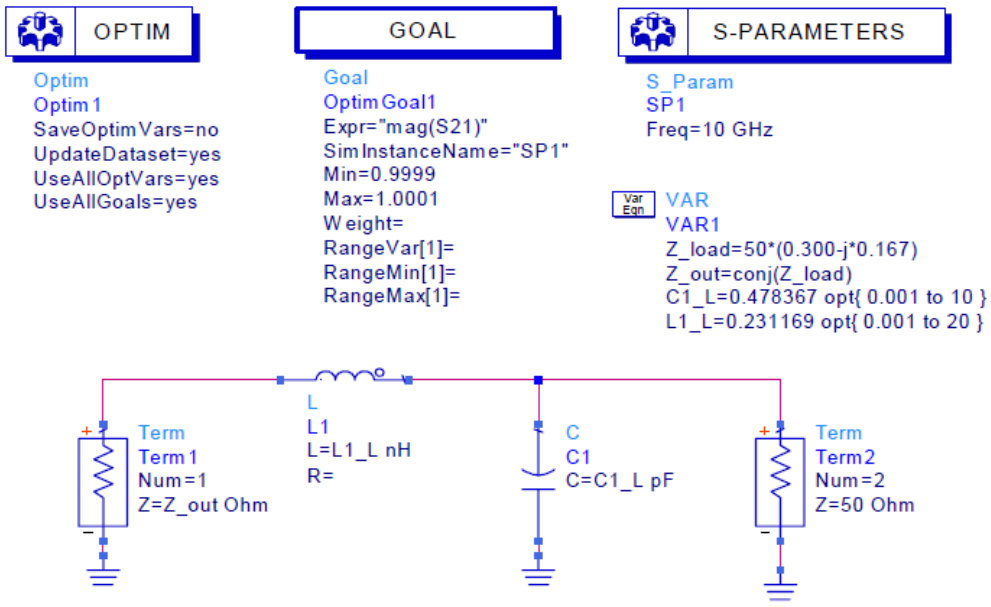

Figure 8.34 Schematic for output matching circuit simulation

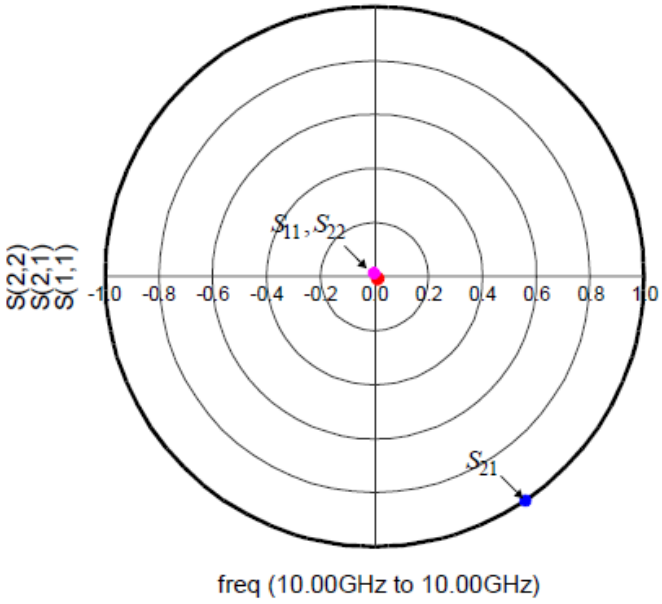

Figure 8.35 Results of the output matching circuits (frequency 10 GHz)

Figure 8.36 is the low noise amplifier circuit configured with the active device and the input and output matching circuits as well as R_{stab} for stability improvement, all configured as subcircuits. The feedback inductor L_e is also included.

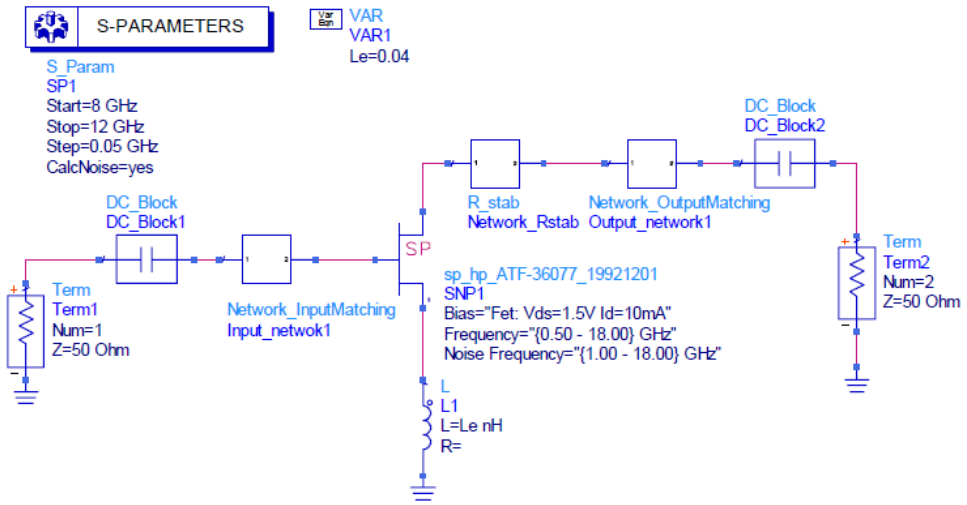

Figure 8.36 The low noise amplifier circuit including Input and output matching circuits

Figure 8.37 is the frequency-dependent S-parameter simulation results for the configured circuit shown above. The gain from Fig. 8.37, is found to be more than 13 dB while the noise figure is below 1.5 dB in the desired frequency band. The difference arising in the gain and noise figure values at frequencies below or above the design frequency is due to the frequency dependences of the matching circuits.

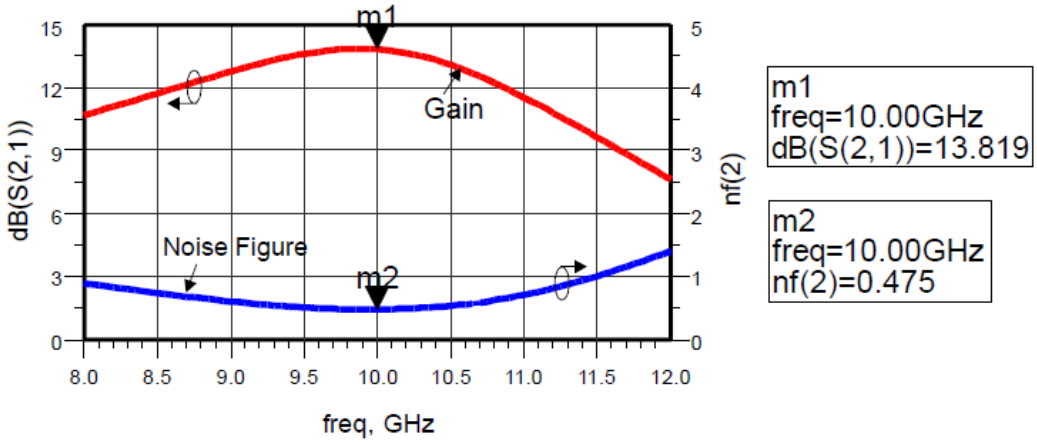

Figure 8.37 Simulation results of the low noise amplifier including matching circuits

8.5.5.2 Transmission Line Matching Circuits

Difficulties in implementation can arise when the lumped-element matching circuit discussed in the previous section is used at high frequency. On the other hand, matching circuit employing transmission lines is easy to implement at high frequency, and in this case, the above design result can easily be obtained by replacing the lumped-elements with transmission line design. In this section, we shall examine matching circuit design using transmission lines.

Figure 8.38 shows the transmission line circuit that can replace the designed lumped circuit. Looking at the relationship between the two circuits, the transmission line with characteristic impedance R_1 and length θ_1 plays the role of L as per equation (8.103a), while the two parallel-connected open transmission lines having characteristic impedance R_2 and length θ_2 play the role of C as per equation (8.103b). It is worth noting that, because the variables of equation (8.103a) are width and length, there are two degrees of freedom in implementing the value of the inductor. The narrower the width, the closer it can be implemented as an inductor, and since the terminals of the inductor are sufficiently wider than that of the packaged active device, there should be no problem in soldering the active device. In addition, the 2 degrees of freedom is also true for equation (8.103b), and the wider the width the better capacitor it is. However, as increasing the width shortens the length, the implemented transmission line circuit appears as two connected transmission lines with step-discontinuity rather than cross-junction connection. To avoid this, the lengths of the transmission lines connected at the cross-junction are made greater than their widths.

$$X_1 = R_1 \tan(\theta_1) \approx \omega L \tag{8.103a}$$

$$X_2 = \frac{R_2}{2\tan(\theta_2)} \approx \frac{1}{\omega C} \tag{8.103b}$$

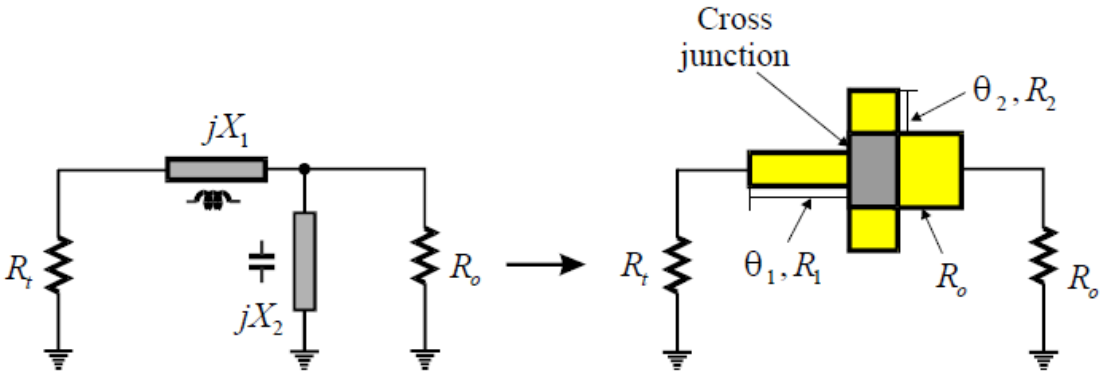

Figure 8.38 Conversion of lumped-element matching circuit to transmission line matching circuit

Since the transmission line connected to the load R_o has the same value of characteristic impedance as the load, the matching circuit has no function when viewed from the load side. However, when an external circuit is connected directly to the matching circuit, the field of the cross-junction shown in Fig. 8.38 may be affected, especially when a coaxial connector is directly connected to the matching circuit. Therefore, the length must be sufficiently long to sufficiently attenuate the higher-order modes arising in the cross-junction.

Figure 8.39 is a schematic for obtaining the input matching circuit constructed from microstrip. As previously explained, the setting of the width and length of the microstrip line provides two degrees of freedom. Of these two, the width is fixed as previously described. The matching circuit is configured by simply changing the length. The width of the transmission line from which the capacitor is implemented is set slightly bigger than the width of a 50 ohm line as **W_C**=1.0 mm; while the width of the transmission line from which the inductor is implemented is set slightly

smaller than the width of a 50 ohm line as **W_L**=0.5 mm. With the widths thus fixed, the length of the two transmission lines, **l_L** and **l_C** are adjusted in a way similar to the lumped-element matching circuit until maximum power is delivered (i.e., until S_{21} is approximately1). Figure 8.40 below is a schematic to determine the input matching circuit composed of transmission line through optimization simulation. The result of this simulation is also shown in Fig. 8.40 together with the schematic; and as can be seen from the results, S_{11} and S_{22} are 0, which indicates impedance matching. Thus, the transmission line matching circuit with these set values can be used in place of the input matching circuit.

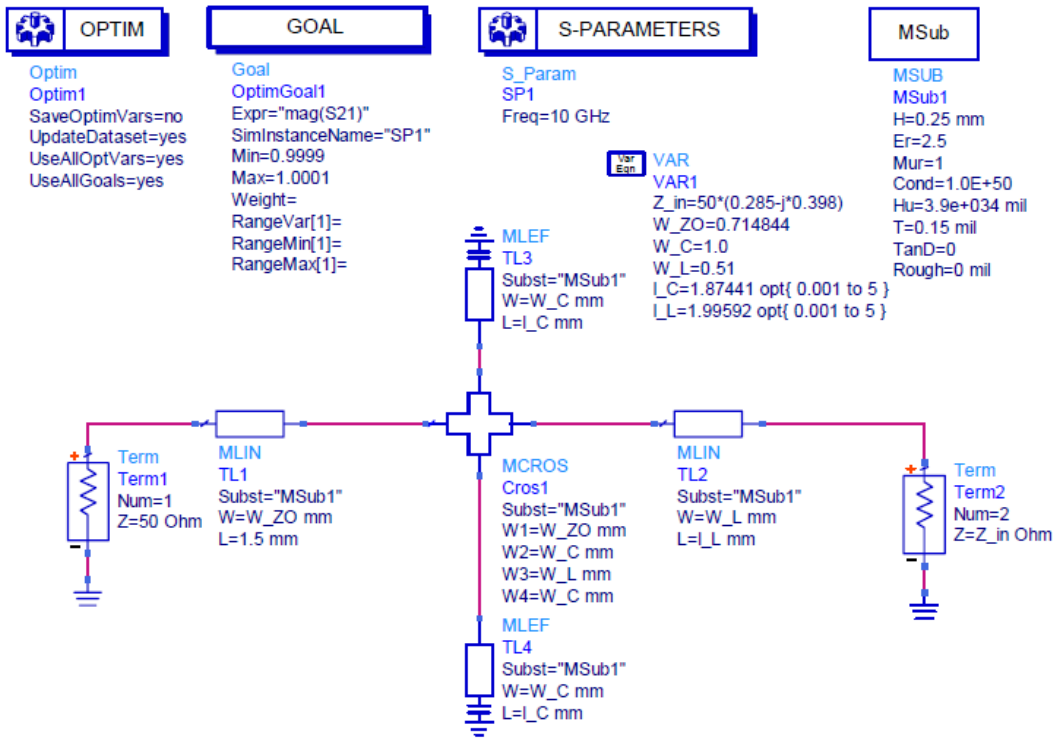

Figure 8.39 Input matching circuit employing transmission lines

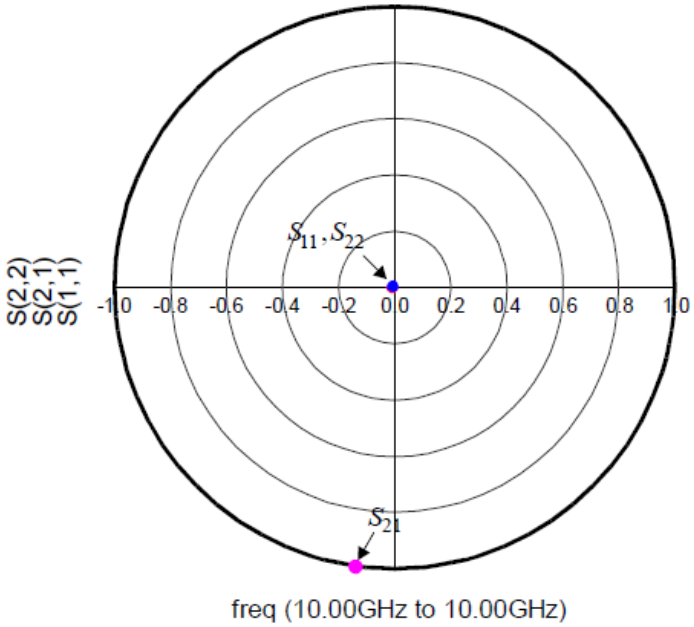

Figure 8.40 Simulation results of transmission line input matching circuit (frequency 10 GHz)

Similarly, for the output matching circuit too, the circuit is set up as shown in Fig. 8.41; and the length of the transmission lines **l_L** and **l_C** were optimized for maximum power transfer. The impedance of port 1 is the complex conjugate of the load impedance while port 2 is terminated in 50 ohm.

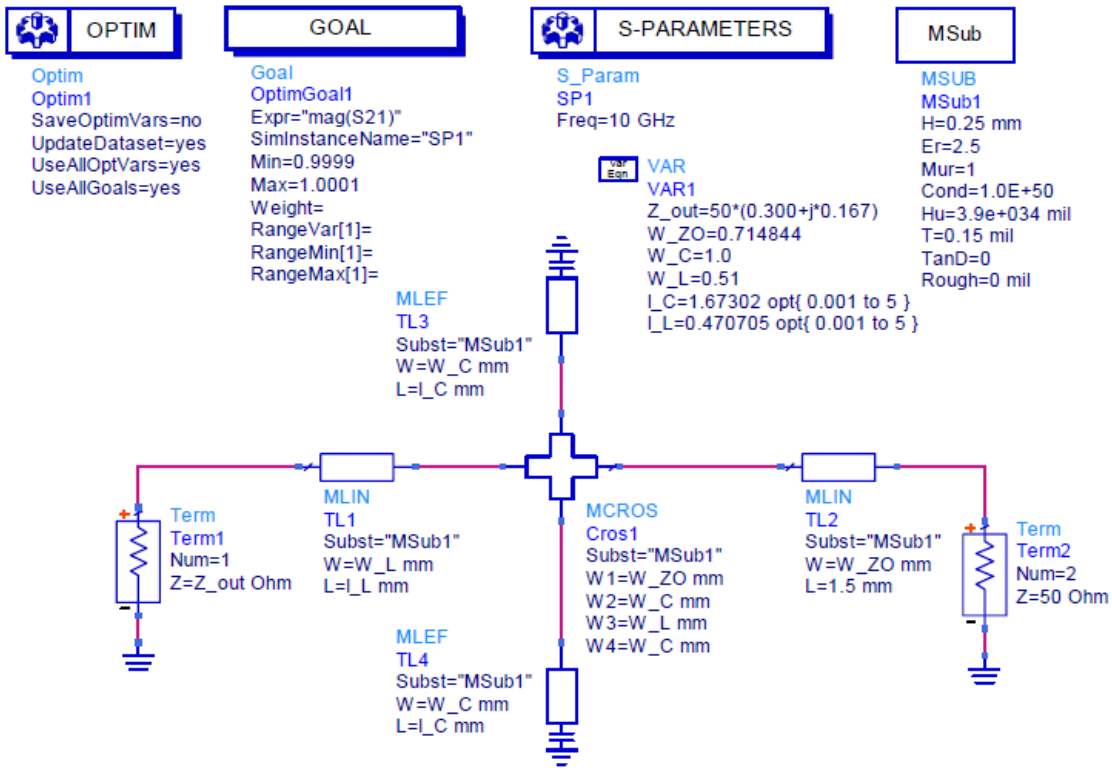

Figure 8.41 Output matching circuit employing transmission lines

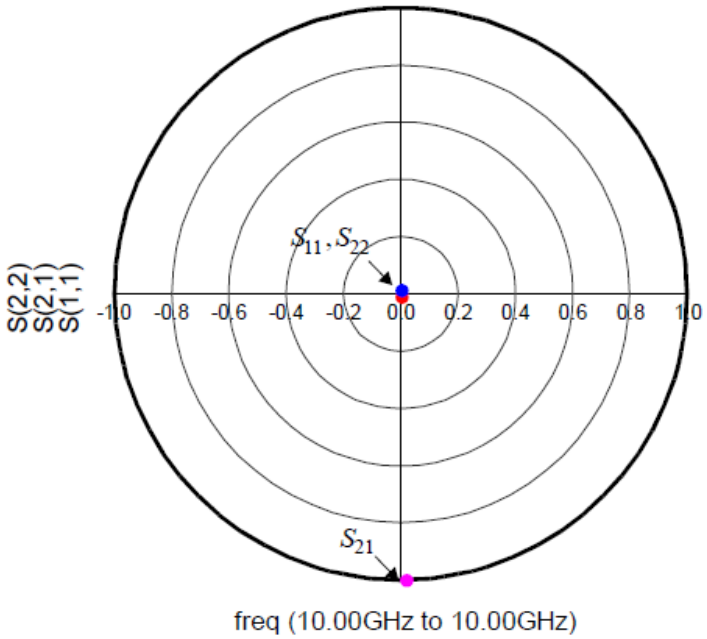

Figure 8.42 Simulation results of transmission line output matching circuit (frequency 10 GHz)

The simulation results shown in Fig. 8.42 are obtained from the circuit of Fig. 8.41. From the results, S_{21} is approximately 1 while S_{11} and S_{22} are approximately 0 indicating proper matching. Thus, the transmission line matching circuit with these set values can be used in place of the output matching circuit.

Figure 8.43 is the simulation results obtained after configuring the input and output transmission line matching circuits as subcircuits replacing the lumped element matching circuits. It can be seen that the expected value of 13.820 dB gain and 0.475 dB noise figure have been achieved. The similarity of this result with the result using the lumped-element matching circuit can also be noticed.

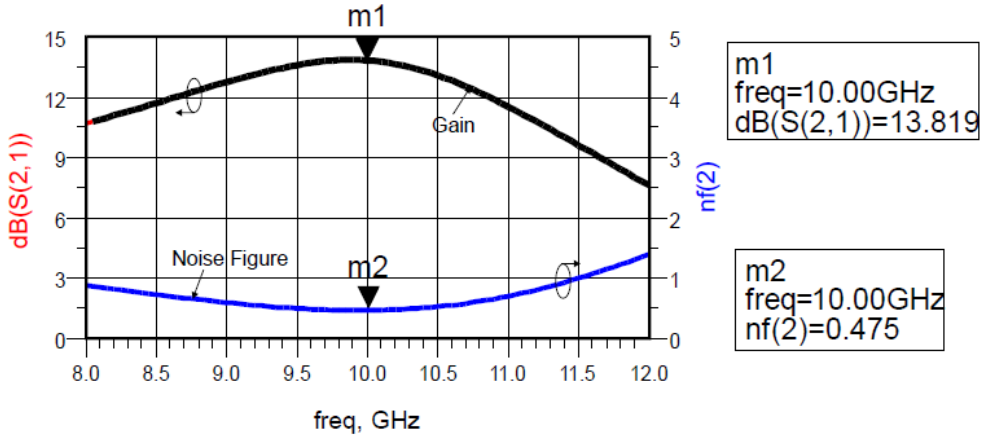

Figure 8.43 Simulation results of the low noise amplifier employing transmission line matching circuits

8.5.6 Addition of DC Supply Circuit

In order to operate the designed low noise amplifier, an appropriate DC voltage must be applied to the active device, and such a DC supply circuit must have as minimal effect on the designed RF matching circuit as possible. In case of any effect, the matching circuit will have to be reconfigured, taking this effect into consideration. In this section, we shall find out about matching circuit design that includes DC supply.

DC block and RFC are usually required to achieve this. It is usually difficult to use chip capacitors as DC block in the current design frequency band due to the parasitic inductance mentioned in Chapter 2. Therefore, the coupled transmission lines shown in Fig. 8.44 are usually used as DC block. However in general, because the coupling of such coupled transmission lines must be close to 1 for a DC block, the spacing between the lines must be very narrow. Therefore, difficult fabrication processes are sometimes required for this DC blocks.

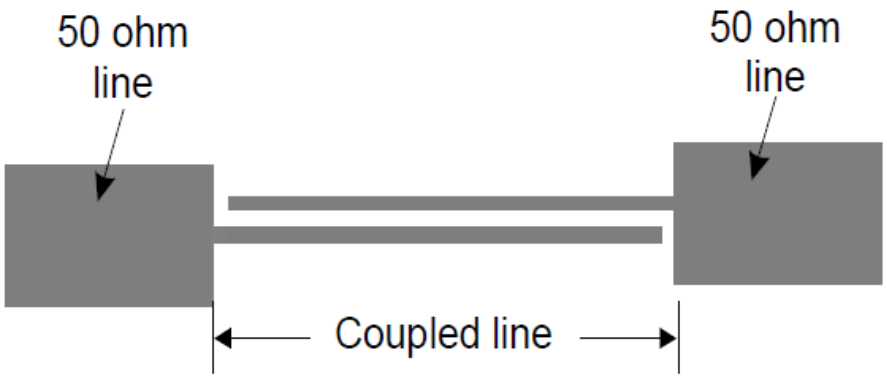

Figure 8.44 DC block using coupled transmission lines

The coupled lines are set up by calculating the S-parameter of the coupled transmission lines shown in Fig. 8.44 with the magnitude of S_{21} being driven to as close to 1 as possible at the center frequency; while the bandwidth is made sufficiently greater than the design bandwidth. The dimensions such as length, width, and spacing are set to satisfy the previous conditions. Note that the results of the matching circuit previously designed can sometimes significantly change due to the DC block and the calculated bandwidth which depends on the frequency characteristics of DC block generally becomes narrower. Since the redesigning of the matching circuit due to the inclusion of the DC block in Fig. 8.44 is similar to the technique of matching circuit redesigning process in the next section, its discussion here will be avoided.

Recently, due to the greatly improved performance of chip capacitors, their use as DC block has become possible and have become widely commercialized [3], [4]. The advantage of the chip DC block capacitor is that it generally does not cause any significant changes to the designed matching circuit compared with the coupled line DC block in Fig. 8.44. In this chapter, we will illustrate a redesigning process of the matching circuit including such DC block capacitor. ATC's 1pF DC block [3] was used in this design and the characteristics of the DC block, which is provided by the manufacturer, is as shown in Fig. 8.45. It can be seen from Fig. 8.45 that, this capacitor operates well as DC block from 5 GHz to 26.5 GHz.

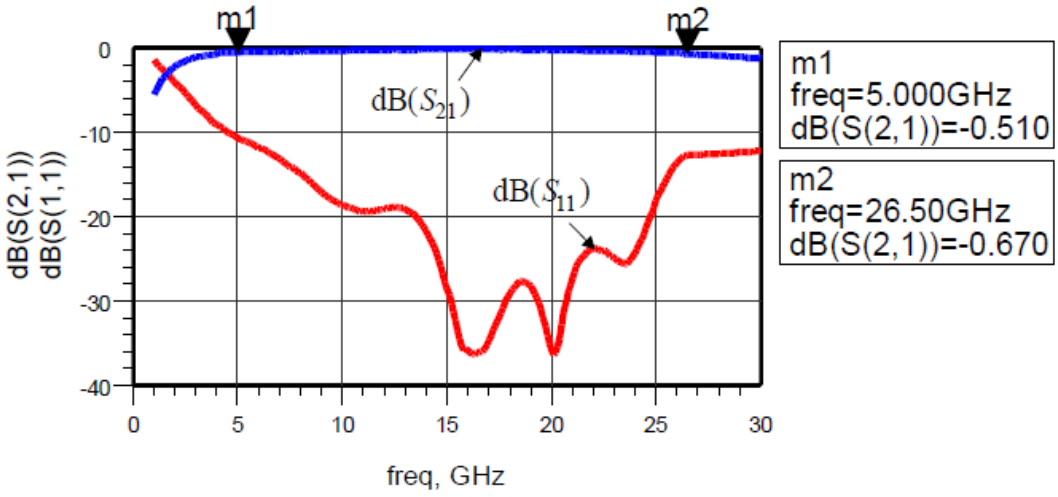

Figure 8.45 The frequency characteristics of 1 pF DC block provided by the manufacturer

As the manufacturer provides the S-parameters of the DC block capacitor in the form of **s2p**, the device can be configured using the **S2P data item** of ADS. This is shown in Fig. 8.46. The obtained simulation result is as shown in Fig. 8.45. It must be noted that, broadband characteristics can be obtained in contrast to normal chip capacitor. Refer to the datasheet for more details on its frequency characteristics.

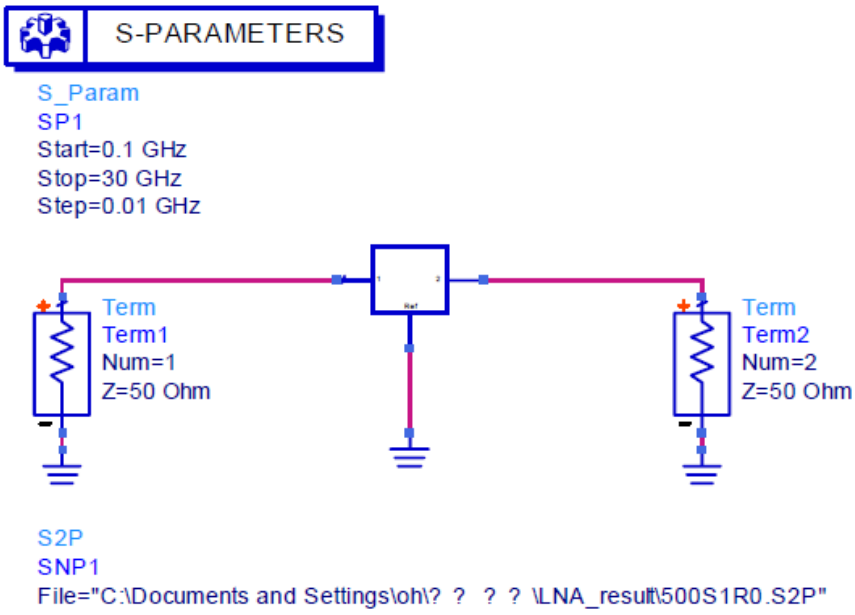

Figure 8.46 DC block capacitor circuit set up

With such a DC block configured as **Data item**, the matching circuit is reconstructed using an RFC consisting of a quarter wavelength transmission line (see Chapter3) as shown in Fig. 8.47 and

the DC voltage of the gate is applied at the connection point of the **MRSTUB stub1**. The transmission line length **I_C** and **I_L** are selected as the optimizing parameters of the matching circuit, as in the case of the previous optimization process.

This is because, the radial open stub and DC block capacitor have effects on the designed matching circuit even though not significant. Thus, it is necessary to carry out new optimization with the DC supply circuit included. Three goals are selected in contrast with the previous optimization. The reason for which is to prevent the possible occurrence of various undesired solutions during optimization.

The other variables mentioned above (the line width and length of the RF choke, etc) are set constant and the simulation is carried out. The simulation results is as shown in Fig. 8.48, where as in the previous case, S_{11} and S_{22} are both 0 while S_{21} is 1, indicating successful matching.

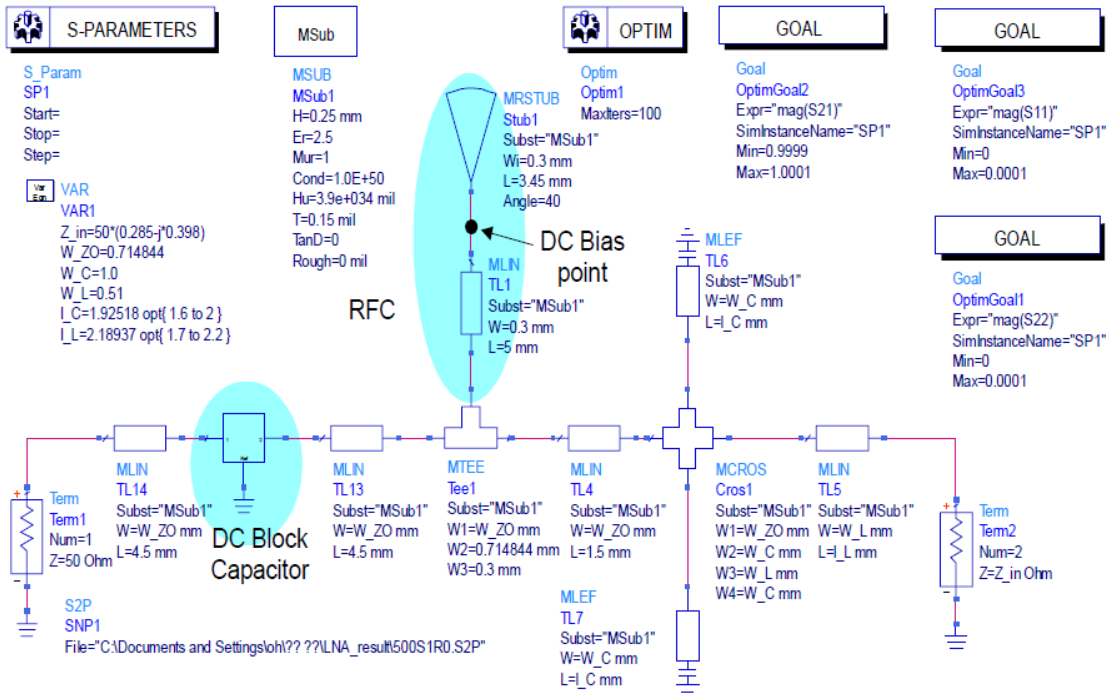

Figure 8.47 Input matching circuit including the DC supply circuit

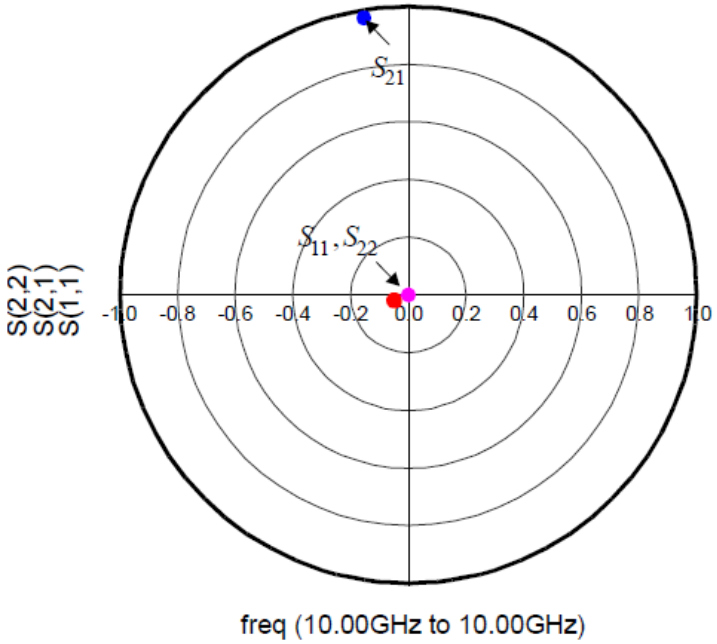

Figure 8.48 Simulation results for the input matching circuit including DC supply circuit

The circuit for optimizing the output matching circuits is set up in the same way as shown in Fig. 8.49. In Fig. 8.49, the drain DC voltage is supplied through a radial open stub as in the input matching circuit. Also the DC block was set up using the data item. The simulation results is as shown in Fig. 8.50; similar to the input matching circuit, S_{11} and S_{22} are both 0 while S_{21} is 1, indicating successful matching.

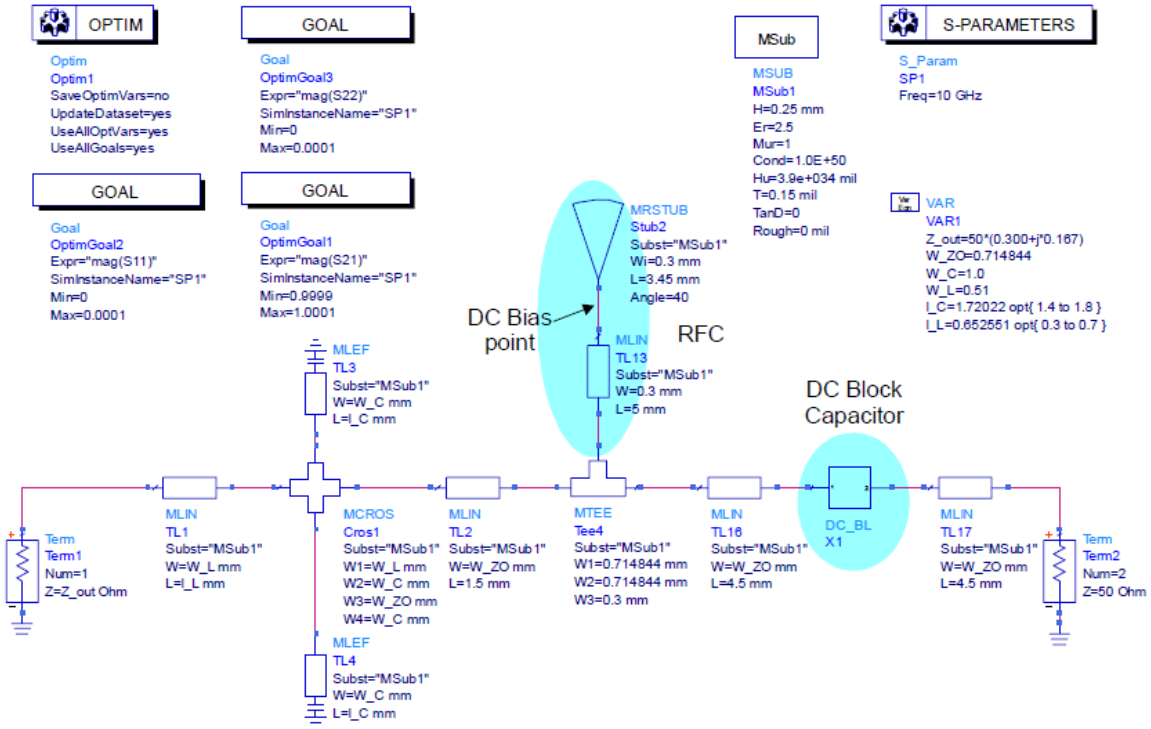

Figure 8.49 Output matching circuit including the DC supply circuit

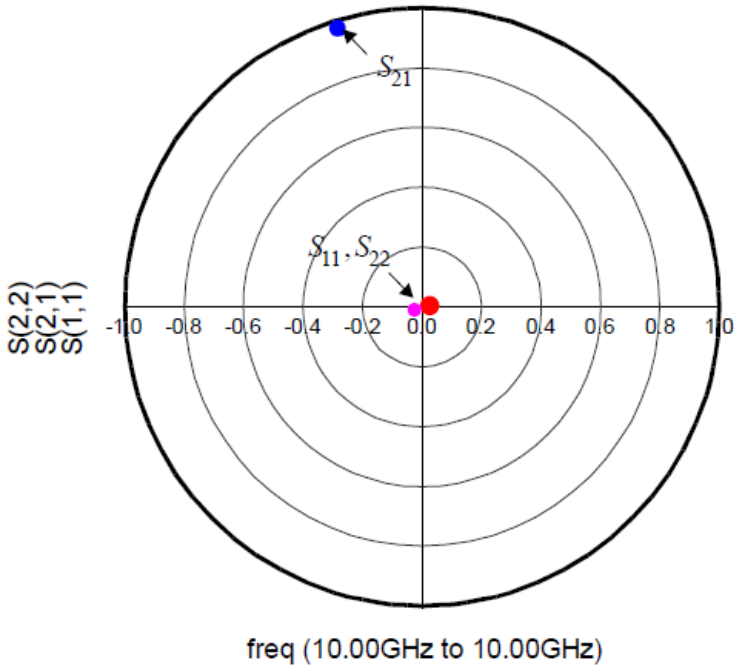

Figure 8.50 Simulation results for the input matching circuit including DC supply circuit

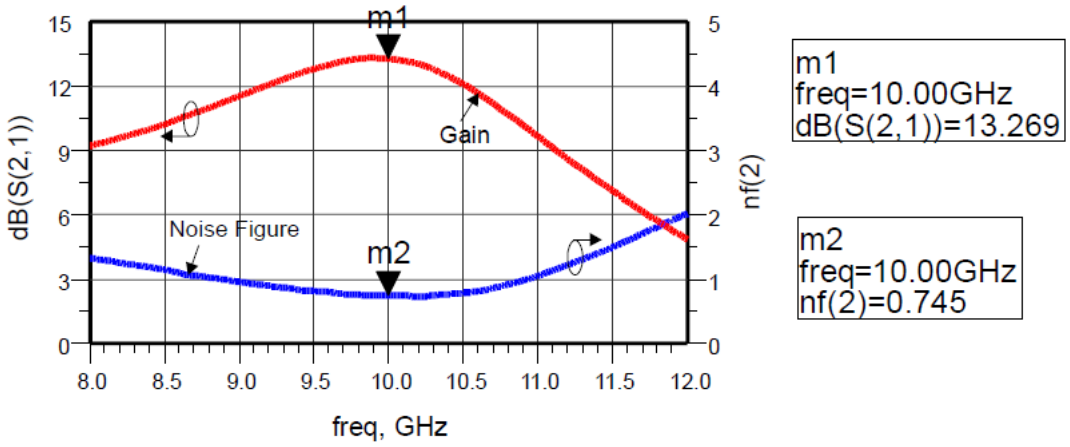

Figure 8.51 Simulation results for the low noise amplifier including DC supply circuit

Figure 8.51 is the simulation result of the low noise amplifier with the input and output matching circuits including DC supply circuit obtained above, configured as a subcircuit for investigating whether the DC supply circuit including the matching circuit is operating correctly. The gain at the desired frequency band is 13.7 dB, which is about 0.1dB less than the result of the low noise amplifier composed only of the matching circuit, while the noise figure is 0.5 dB increasing by approximately 0.2 dB. This is believed to be due to the loss in the DC block capacitor.

8.5.7 Stability Check

The stability of the designed low noise amplifier should be checked at low frequencies at the final stage of the design. To investigate the stability, the matching network impedances Γ_S and Γ_L looking into the source and load from the transistor is plotted on the Smith chart together with the frequency-dependent source and load stability circles. It can then be determined whether Γ_S and Γ_L for each frequency lie in the stable region. Alternatively, new S-parameters are defined for the entire low noise amplifier circuit, and then its frequency-dependent stability can be investigated. In this case, the source and load stability circles are defined by the newly defined S-parameters in which case the source and load impedances Γ_S and Γ_L become the port impedances resulting in $\Gamma_S=\Gamma_L=0$. Therefore, since the change of source and load impedances with frequency needs not to be considered, then the investigation is by determining whether the origin of the Smith chart is in the stable region at each frequency.

In the latter method, since the source and load stability locus is $\Gamma_S=\Gamma_L=0$, the origin on the Smith chart, determining whether the origin is in the stable region or not is much easier compared to the former method of checking the stability at the plane of the active device. In addition, repeatedly determining whether it is stable or unstable at each frequency is visually much easier in the latter method.

Other problems include making sure that Γ_{in} and Γ_{out} for the selected Γ_S and Γ_L do not become negative resistances. Therefore, $|\Gamma_{in}|<1$ and $|\Gamma_{out}|<1$ must be satisfied for the selected Γ_S and Γ_L. In this case, for the newly defined S-parameters of the amplifier, $\Gamma_{in}=S_{21}$ and $\Gamma_{out}=S_{22}$ and so $|S_{11}|<1$ and $|S_{22}|<1$ must also be satisfied. Therefore, investigation of low-frequency stability as per the S-parameters defined for the amplifier is:

1) To investigate the frequency range in which the origin is unstable

2) To investigate the frequency range in which $|S_{11}|>1$ and $|S_{22}|>1$, in which case the matching circuit has to be re-adjusted until these undesired conditions disappear.

Figure 8.52 is the designed low noise amplifier circuit with the matching circuit. We now investigate the frequency-dependent stability behavior of the matching circuit.

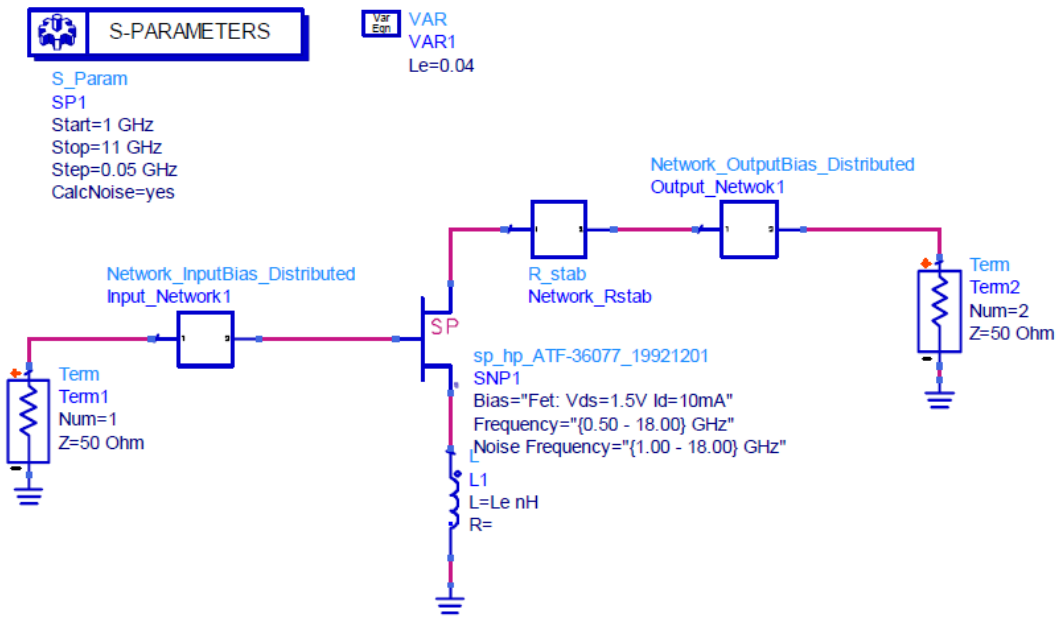

Figure 8.52 Circuit set up for investigating low frequency stability

The circuit of Fig. 8.52 is set up to investigate stability at frequencies other than the design frequency. After S-parameters simulation, the stability circle function is defined in the Display window and the frequency-dependent input and output stability circles can be plotted as shown in Fig. 8.53. In addition, the stable region can be known by using the ADS stability region investigation function (see Example 8.2). These results are shown in Figs. 8.53(a) and (b). Also, the input and output reflection coefficients Γ_{in} and Γ_{out} become S_{11} and S_{22} respectively since the input and output are both terminated in 50 ohm load; which is also shown in Fig. 8.53.

In Fig. 8.53(a), the stable regions are outside except at the 1 GHz frequency. On the other hand, it can be seen that, instability occurs at 1 GHz. Also, in Fig. 8.53(b) all the frequencies are stable, but since the reflection coefficient S_{11} seen from the input of the transistor is larger than 1, instability occurs.

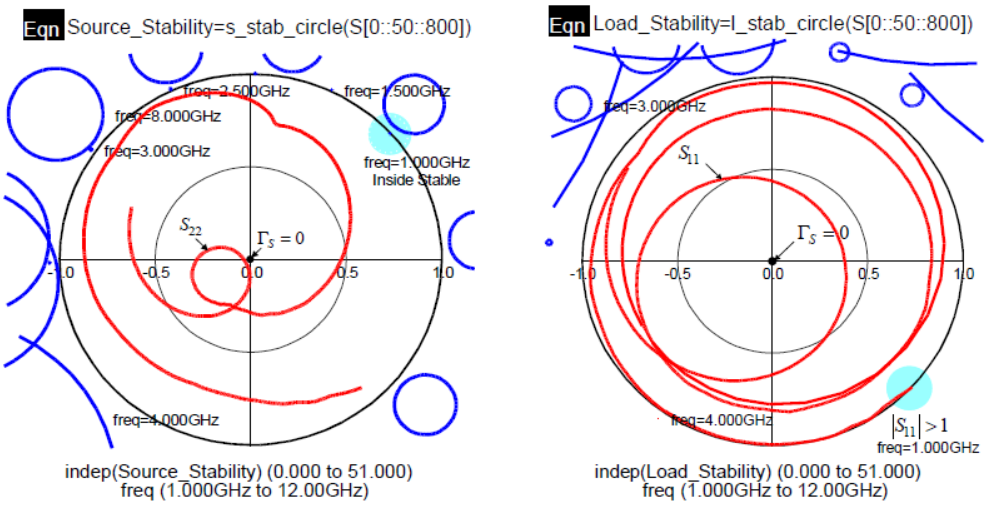

(a) (b)

Figure 8.53 Results of low-frequency stability investigation

From these results, as the magnitude of the output reflection coefficient S_{11} is greater than 1 at 1 GHz, it can be seen that a negative resistance appears at the output. The reason for the appearance of this negative resistance at low frequencies could be attributed to the DC block inserted in the DC supply of the input matching circuit in Fig. 8.52, which becomes open at low frequency. Therefore in order to remove this effect, the input as well as the matching circuit is made to appear as close to 50 ohm as possible at low-frequency which solves the problem. Considering that, the gate of the FET draws no DC current; a resistor of 50 ohms inserted in series with the DC supply circuit will have no effect on the DC voltage. On the other hand, as the drain draws a considerable current, inserting a resistor could change the operating point. Therefore, a 50 ohm series resistor is inserted in the input as shown in Fig. 8.54. Note that, the DC is supplied through the capacitor C_1.

This method seems somewhat a trial and error approach and yet, it is a commonly used method. Usually, the S-parameters of most active devices are measured using 50 ohm measurement reference impedances and the devices are stable in most cases. Also the S_{11} or S_{22} of active devices is usually less than 1 for most cases. Therefore, for any frequency at which the active device is unstable, making the impedance seen from the active device into the source or load close to 50 ohm at that frequency will make the active device as stable as when it was measured. In this sense, the impedance seen from the active device is made close to 50 ohm at low frequencies. Most stabilizing circuits can essentially be seen to be the application of this concept. It is worth noting that, the insertion of these resistors can affect the DC voltage or the flow of current, and this must be prevented when inserting the resistors.

The newly defined S-parameters of the amplifier is simulated using the input matching circuit thus modified as shown in Fig. 8.54; with the same circuit used for the output matching circuit. These results are shown in Fig. 8.55. As can be seen from Fig. 8.55, the stability circles at all frequencies are located outside the unit circle and the region in the unit circle is found to be the stable region. In addition, both input and output reflection coefficient S_{11} and S_{22} can also be seen to lie in the unit circle.

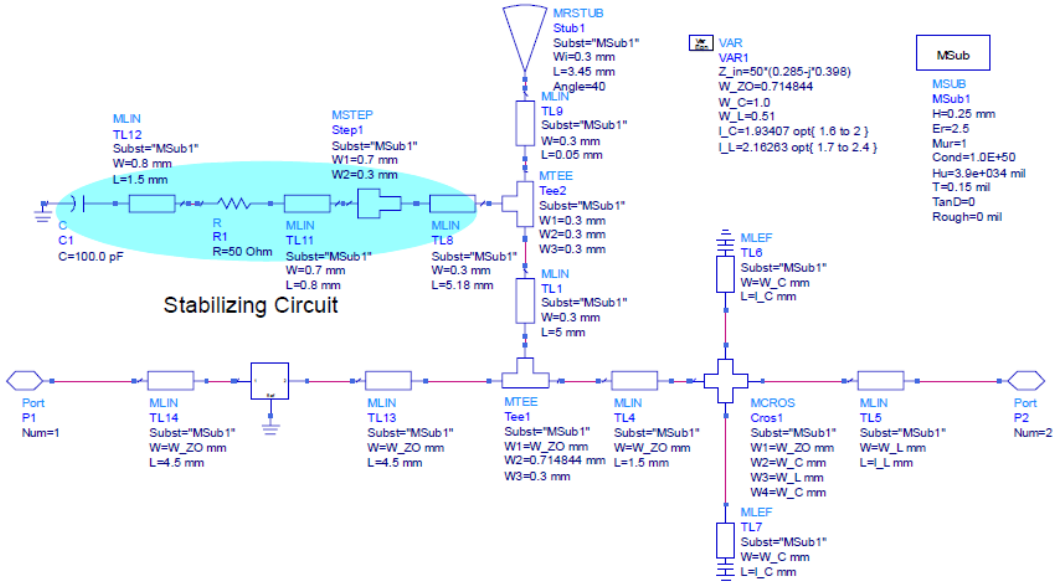

Figure 8.54 Solutions of low frequency source stability problem using a resistor

In conclusion, low-frequency instability, as mentioned earlier, is solved by inserting a resistor in the DC supply circuit, which must carefully be done in order not to affect the circuit at the design frequency. In this way, the instability at low frequencies can mostly be eliminated. At the same time, care must be taken so that the DC voltage or current flow is not affected.

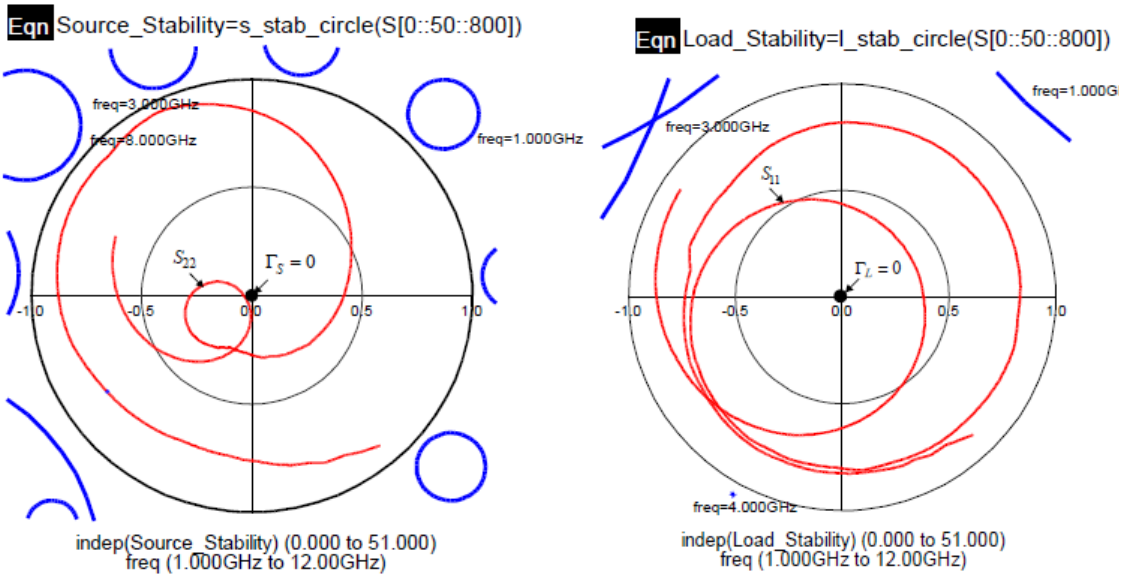

Figure 8.55 Results of low-frequency stability investigation

8.5.8 Fabrication and Measurements

A layout of the previously designed low noise amplifier is required in order to fabricate the amplifier. It is necessary to perform EM simulation before the layout is carried out in order to reduce trial and error. Firstly, the task of implementing the feedback inductor pattern at the design frequency, which is connected to the actual source terminal, is required and so is its confirmation. Next, the matching circuit pattern needs to be confirmed through momentum simulation.

8.5.8.1 Feedback Inductor Design

So far the simulation was carried out considering the source inductor as only an ideal lumped component. It is necessary to convert this to a distributed circuit using transmission line circuits. A careful consideration is required for the selected inductance which is designed using transmission line via, as it is an important element that determines the overall stability of the circuit. Its characteristic is that, it should be a short to DC and an inductor to RF. When these circuits are implemented using transmission lines, it is preferable to short it through a via at the end of the transmission line. Since a via has self-inductance, it is especially important to verify the via through momentum EM simulation in order to determine it more precisely. The via compliant to manufacturing standard is shown in Fig. 8.56. The determination of the standard depends on the capability of the manufacturers.

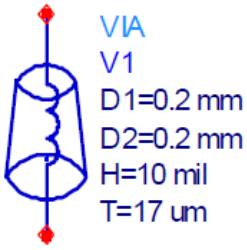

Figure 8.56 via used in the design

The inductor circuit in Fig. 8.57 is set up in the Schematic window using vias and transmission lines. The ATF-36077 transistor is configured with two source terminals, and in order to apply the inductor design simultaneously at two places using a via, the designed inductor using transmission lines and via must have 2 times the value of a single inductor which is 0.08 nH.

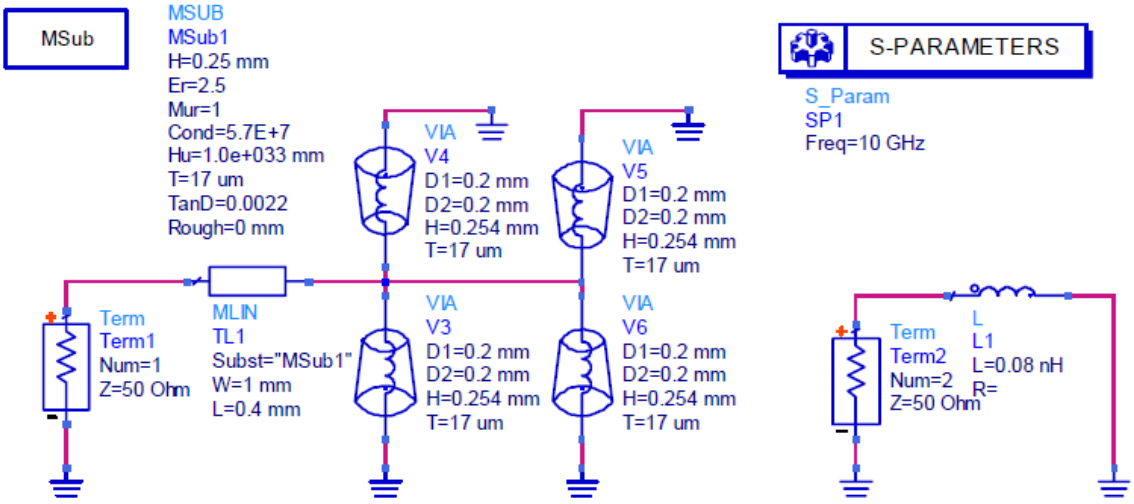

Figure 8.57 Inductance circuit implement using transmission lines and via

In Fig. 8.57, the inductor on the right is for the representation of the simulation result of the designed inductor value on the Smith chart, which enables comparison with the results of the simulation on the left. The value of the implemented inductor on the left is obtained by varying the length of the transmission line **TL1**. The value of the length of transmission line thus obtained is shown in Fig. 8.57. The number of vias being 4 is, one of the via has inductance in excess of 0.08 nH, which makes it possible to adjust the inductance through the transmission line by reducing the via dependent inductance. With the simulation result of Fig. 8.57, the circuit with the desired inductance could be configured and the length of the transmission lines could also be used as the pad of the source terminal.

The auto-layout feature of ADS is used to automatically generate the layout of the designed circuit to be verified using momentum. The Layer settings can easily be configured in the Layout window by importing the **MSUB** information in the Schematic window. Figure 8.58 is the result of the layout of Fig. 8.57.

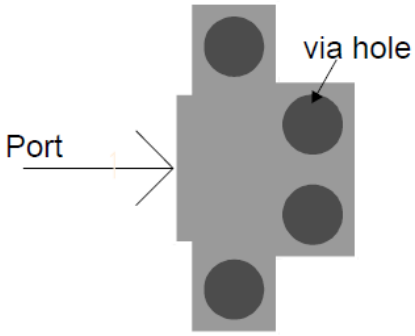

Figure 8.58 Layout implementation of the inductance circuit using transmission lines and vias

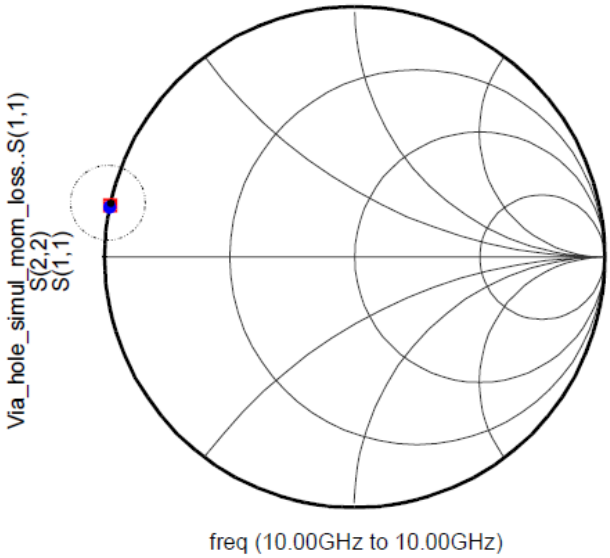

Figure 8.59 Comparison of inductance results obtained from circuit and momentum simulation

A slight difference between the Momentum simulation result and the circuit simulation results can be noticed, this is due to an increase in the electrical length caused by parasitic elements at the design frequency of 10 GHz which extends the inductance beyond the set value. Considering this, the inductor value can be corrected to 0.08 nH by adjusting the length of the transmission line to be shorter than that in the layout.

Figure 8.59 shows the comparison results of the inductance and circuit simulation after the length adjustment. It can be seen that, the inductance value of the lumped circuit, distributed circuit, and momentum results show good agreement.

8.5.8.2 Modification of the Matching Circuits

The transmission lines and the PCB used in the actual fabrication have inherent losses in the dielectric of the substrate material as well as conductor losses coming from the surface and thickness of the conductor. These are losses not considered in the characteristics of the

previously designed low noise amplifier circuit. These loss factors are considered in ADS simulation and after confirming the results, some slight modifications may be necessary. Loss consideration is particularly necessary due to the deterioration of the noise figure in the implementation of the low noise amplifier arising from losses at the front end of the active device. Firstly, it is possible to include losses through the settings of **MSUB** from the circuit simulation of the ADS Schematic window. Items to consider in **MSUB** and their corresponding values are summarized in Table 8.4. The entered values here are for Rogers' UL2000; the reader may refer to [5] for the corresponding product data.

Table 8.4 PCB substrate information

NO.	Item	MSUB_menu	Value
1	Conductor thickness	T	17 um
2	Conductivity	Cond	5.8×10^{7} S/m (Copper)
3	Loss tangent	TanD	0.0022

After considering these losses, the matching circuits are again re-designed to optimize their values. The detailed circuit configuration is the same as the previously designed structure; only the length of a part of the matching circuit needs to be slightly modified. The substrate in this condition is still not quite accurate when considered as a circuit. Therefore, in order to investigate the matching circuit using momentum, the layout is configured with the additional elements connected to the DC blocks and RFC all removed. The reason for removing these elements is that, their effect cannot be considered in momentum and the effect of DC supply circuit connected after the RFC is also small at the design frequency. The layout of the input and output matching circuits are generated using ***Auto-Layout*** and EM simulation is then performed using ***Momentum***. Figure 8.60 shows the layout of the considered input matching circuit. Due to unknown effects which cannot be considered in circuit simulation, the result of the momentum EM simulation is slightly different from the results obtained from circuit simulation.

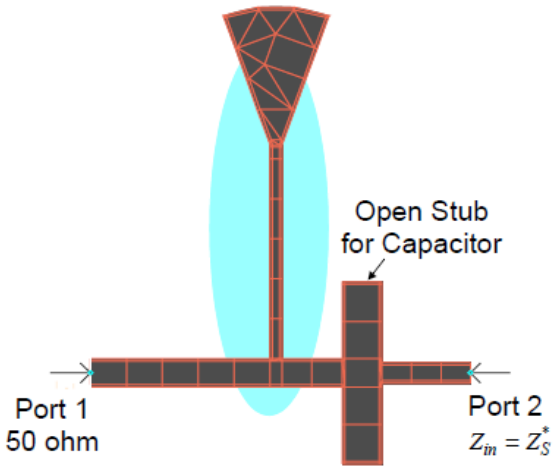

Figure 8.60 Layout configuration for the momentum simulation of the input matching circuit without DC block

Figure 8.61(a) shows the comparison of the two impedances seen from the input of the device; one for the circuit simulation results and the other for the momentum simulation results of the input matching network. Figure 8.61(b) shows the two results of the output matching circuit.

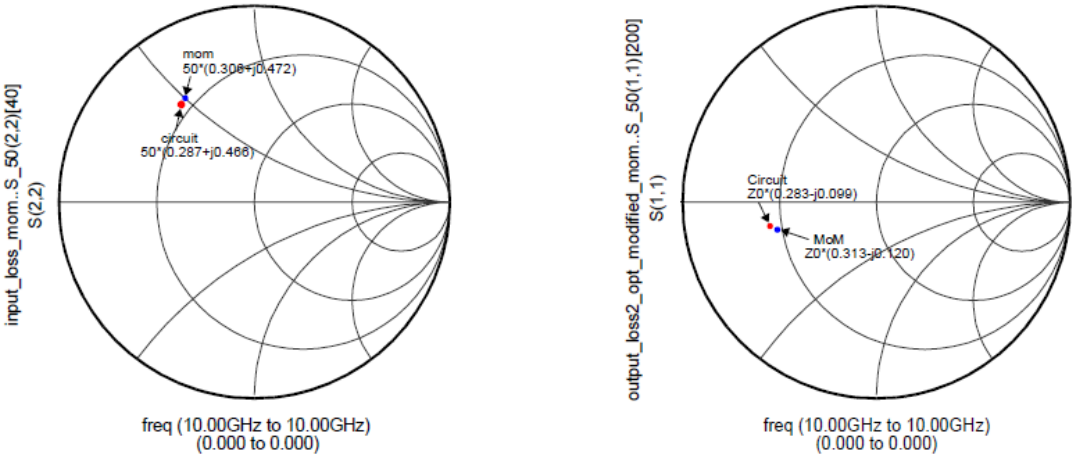

(a) (b)

Figure 8.61 Circuit simulation results compared with momentum for (a) input and (b) output matching circuit at 10 GHz frequency

The difference arises largely from replacing the lumped element capacitor in the matching circuit with the open stub. Thus, the desired impedance can be obtained by shortening the length of the stub. Reducing the length of the open-stub for the input matching circuit by 0.15 mm on both sides of the open stub; and for the output matching circuit, by 0.1 mm, yield the values of the impedances obtained from circuit simulations. Figure 8.62 shows the comparison results for the input and output matching network after the adjustments in the lengths.

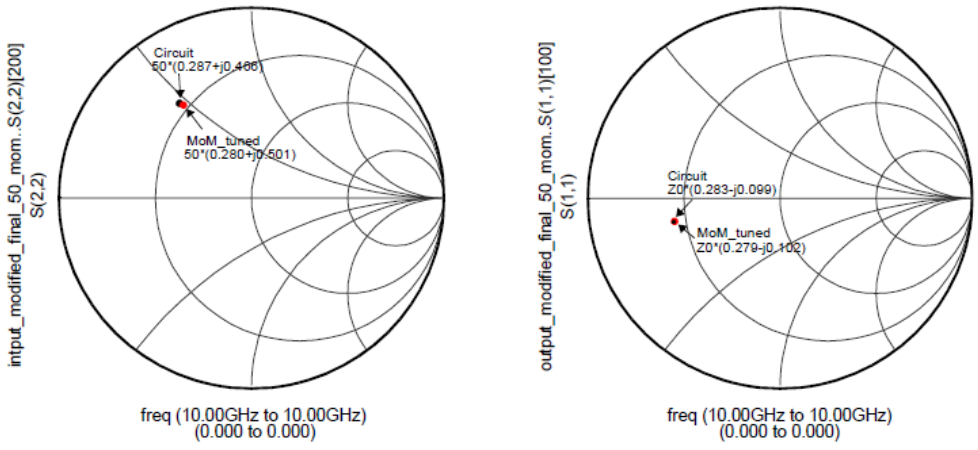

(a) (b)

Figure 8.62 Compared results for (a) input and (b) output matching circuit at 10 GHz after length adjustments.

It is necessary to perform simulations using the EM simulation results to verify whether the obtained momentum results give the desired characteristics of the low noise amplifier. The matching circuit simulation results obtained from momentum as well as the result of the via analysis can be imported as circuit using data item of the Schematic window. The DC Block, provided by the manufacturer as previously explained, is also included as data item in the simulation. Figure 8.63 is the circuit set up for confirming the low noise amplifier designed using data item.

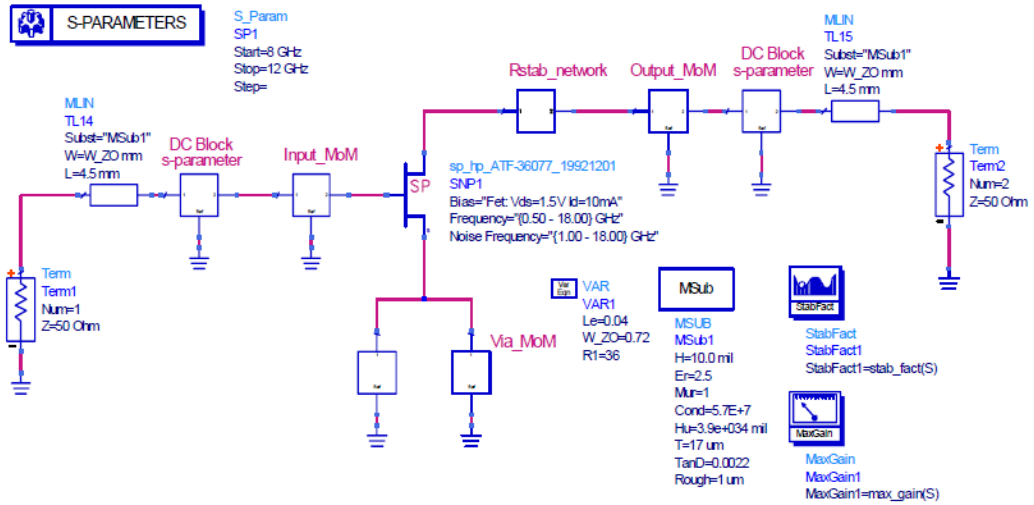

Figure 8.63 Circuit for low noise amplifier characterization using Data item

Figure 8.64 is the simulation result of the circuit thus configured. From Fig. 8.64, the gain is found to be more than 12 dB and the noise figure, less than 1.5 dB which satisfies the design specifications in the design frequency band. Comparing this with the previous results, it can be seen that, gain has decreased while the noise figure has increased; this is due to the substrate loss factors included in the momentum simulation. In addition, the change in the length of the open stub which was made from the previously designed transmission line must be noted.

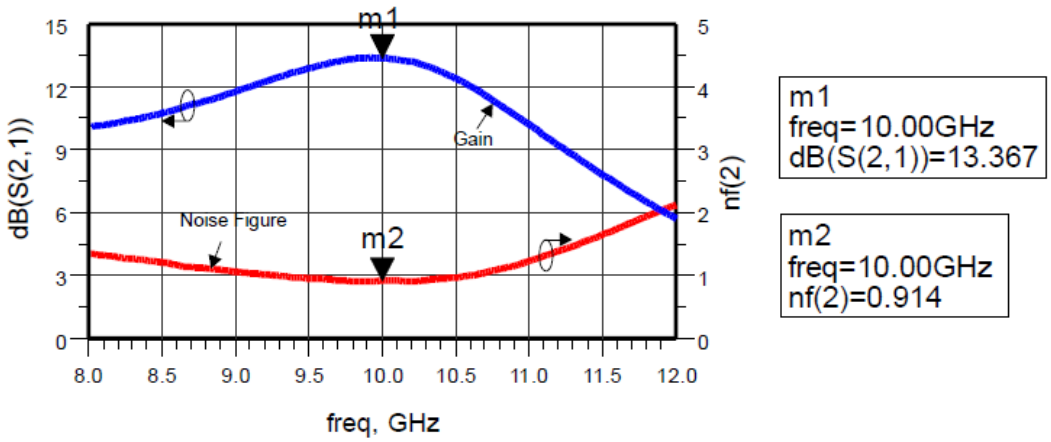

Figure 8.64 Results of Momentum simulation gain and noise figure with DC block included

8.5.8.3 Fabrication and Measurement

The low noise amplifier is fabricated based on the above simulation results. The substrate used in the fabrication is the Rogers's UL2000 substrate considered in the simulation which is 10 mil thick and has a dielectric constant of 2.5. ATC's 1pF broadband 0603 type 500L is used as the DC block capacitor. In addition, the gate bias is applied at the back of the100 pF capacitor after a 51 ohm chip resistor and a 100 pF capacitor were attached to the gate bias of the low noise amplifier. Next, for the overall stability of DC supply, a 3.3 µF capacitor was connected to the input of the gate and drain bias.

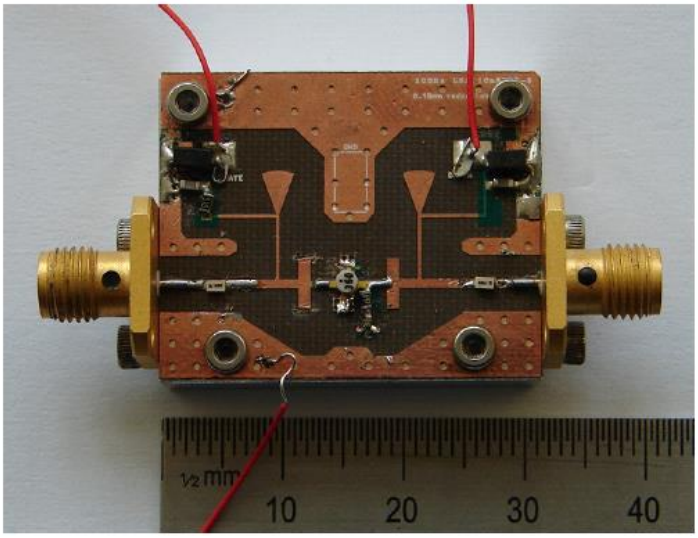

Figure 8.65 The fabricated 10 GHz low noise amplifier

Figure 8.65 is the photograph of the actually fabricated low noise amplifier. During measurement, the nominal gate bias voltage is adjusted until the rated drain current flows.

With gate voltage V_{gs}=−0.33 V, the drain current flowing is found to be near a nominal value of 10 mA. The drain current then was 10.7 mA.

The noise figure and gain were measured using a Noise Figure Analyzer (NFA). In measuring the noise figure of the low noise amplifier, an attenuator is typically inserted at the front-end of the amplifier. That is, since the internal function of the NFA can compensate the used attenuator, the NFA is calibrated with the attenuator inserted. This is done to reduce the mismatch between the low noise amplifier and the noise source. After the calibration, the noise figure and gain of the low noise amplifier is measured. Slight deviation from the simulation results is observed and this was tuned by decreasing the stub lengths.

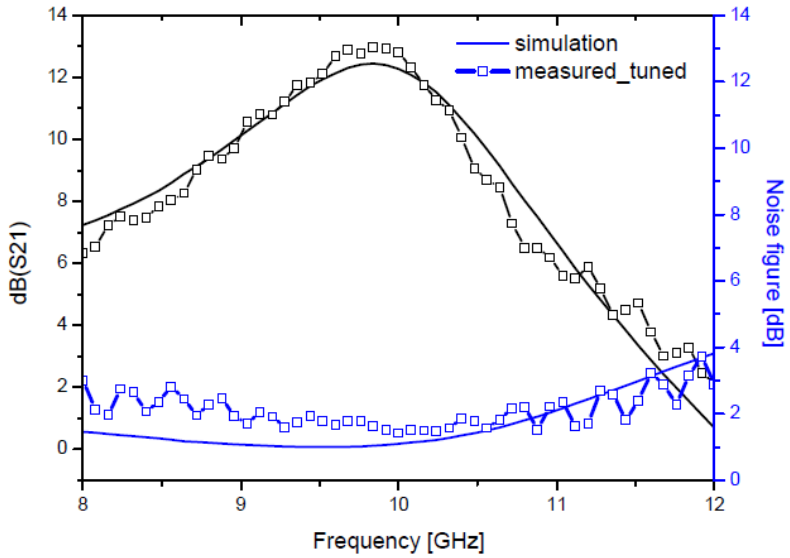

Figure 8.66 Measurement results of 10 GHz LNA

Figure 8.66 is the noise figure and gain respectively for the optimized low noise amplifier. With a noise figure of 1.42 dB (design goal <1.5 dB) and gain of 12.8 dB (design goal> 10 dB) at 10 GHz, it can be seen that this satisfies the design specifications. The simulation results give noise figure of about 0.9 dB and gain of 13.4 dB; it can however be seen that, while the measured gain is optimized, the noise has increased. This is believed to be due to the effect of the connectors which were not considered in the simulation.

In order to determine the cause of the increase in noise, a test jig was constructed with the same length of 50 ohm transmission line connecting the two connectors. Evaluating this loss will help us predict to what extent the increase in noise is due to the connectors. Figure 8.67 shows the measured results. In Fig. 8.67, the loss is −1.24 dB at 10 GHz, which explains the slight increase in the noise figure at the design frequency. This can be considered as reflections due to mismatch, but it can be seen from Fig. 8.67 that, the return loss within the entire band is less than 10 dB. Therefore, the increase is found to be due to connector and microstrip line losses. Considering this as connector loss and calculating, the noise figure is 1.5 dB (= 0.88 + 1.24 / 2) which explains the experimental results. That is, this can be considered as the degradation in noise characteristics of the low noise amplifier due to connector loss.

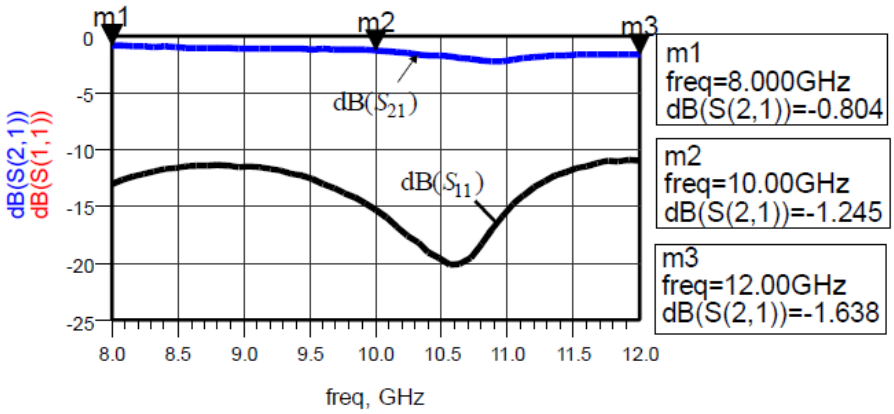

Figure 8.67 Results of connector loss measurement

REFERENCES

[1] G. Gonzalez, *Microwave transistor amplifiers*, 2nd edition, Prentice Hall, 1997.

[2] D. M. Pozar, *Microwave Engineering*, 2nd edition, John Wiley & Sons Inc., 1998.

[3] American Technical Ceramics, *ATC 500S Series BMC Broadband Microwave Millimeter-wave 0603 NPO SMT Capacitors*, Available at http;//www.atceramics.com

[4] American Technical Ceramics, *ATC 545L Series UBC Ultra-Broadband Capacitor*, Available at http;//www.atceramics.com

[5] Rogers corporation, *ULTRALAM2000 HF laminate*, Available at http;// www. rogerscoporation.com

PROBLEMS

8.1 Prove equation (8.25) using the input reflection coefficient of the active device.

8.2 Derive the power delivered to the load Γ_L in the circuit shown below for which measurement was carried at 50 ohm reference impedance.

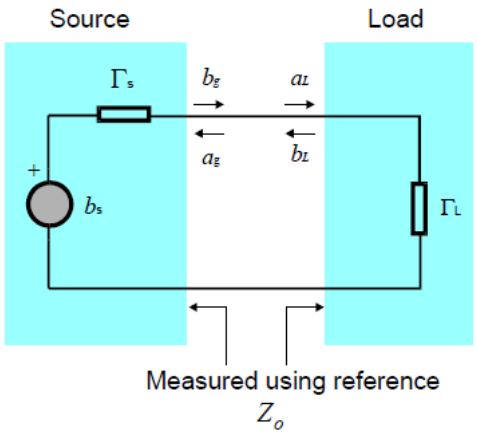

Figure 8P.1 Circuit connection of load (as reflection coefficient) to a source

8.3 Determine the Thevenin reflection coefficient, Γ_T of the following circuit when the circuit is represented by Thevenin equivalent circuit in a 50 ohm measurement reference.

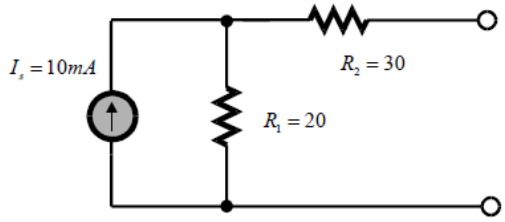

Figure 8P.2 Circuit with source and internal resistance

8.4 Answer each of the following questions for the circuit below.

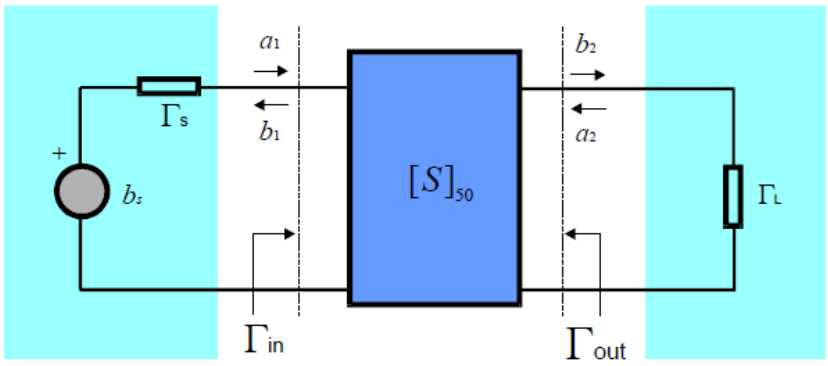

Figure 8P.3 Low Noise Amplifier configuration

(1) Derive the transducer power gain
(2) Derive the available power gain

8.5 The available power from the source, by way of a different approach to deriving the available power gain when $\Gamma_S = (\Gamma_{in})^*$ as previously discussed, is as given below:

$$P_{Ai} = \frac{|b_s|^2}{1-|\Gamma_s|^2}$$

In addition, the available power in the load from the output of the active device in the Thevenin equivalent circuit is expressed as follows:

$$P_{Ao} = \frac{|b_T|^2}{1-|\Gamma_{out}|^2} = \frac{|b_s|^2 |S_{21}|^2}{|1-S_{11}\Gamma_s|^2 |1-\Gamma_{out}|^2}$$

Using these equations; show that the available power gain is given by:

$$G_A = \frac{P_{Ao}}{P_{Ai}} = \frac{\left(1-|\Gamma_s|^2\right)|S_{21}|^2}{\left(1-S_{11}|\Gamma_s|^2\right)\left(1-|\Gamma_{out}|^2\right)}$$

8.6 The power gain is the fraction of the input power delivered to the load; in other words, it is determined as the ratio of the power delivered to the load to the input power when the input is matched for maximum power transfer. Therefore, for a given transducer power gain, maximum power is transferred to the load when the source impedance is conjugate matched to the input impedance.

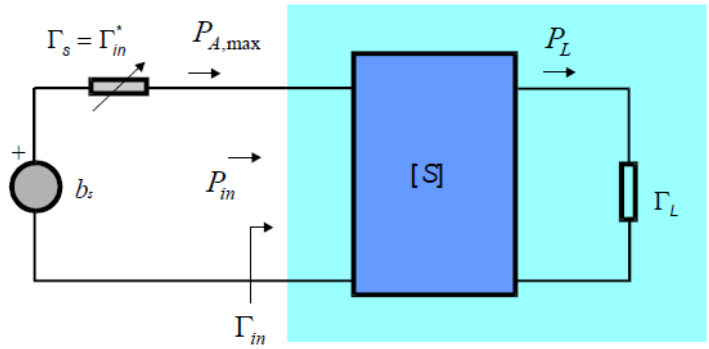

Figure 8P.4 Another interpretation of power gain

Derive the following expression when the $\Gamma_s = \Gamma_{in}^*$ condition is satisfied,

$$G_T = \frac{P_L}{P_A} = \left.\frac{\left(1-|\Gamma_s|^2\right)|S_{21}|^2\left(1-|\Gamma_L|^2\right)}{|1-\Gamma_{in}\Gamma_s|^2|1-S_{22}\Gamma_s|^2}\right|_{\Gamma_s=\Gamma_{in}^*} = \frac{|S_{21}|^2\left(1-|\Gamma_s|^2\right)}{\left(1-|\Gamma_{in}|^2\right)|1-S_{22}\Gamma_s|^2}$$

8.7 The input reflection coefficient is expressed as follows,

$$\Gamma_{in} = S_{11} + \frac{S_{12}S_{21}\Gamma_L}{1 - S_{22}\Gamma_L} = S_{11} - \frac{S_{12}S_{21}}{S_{22} - \dfrac{1}{\Gamma_L}}$$

Given that, in this equation, $\Gamma_L = e^{-j\theta}$ (assuming a unit circle of magnitude 1), prove that this is a circle with center and radius given below:

$$C_L = S_{11} + \frac{S_{12}S_{21}S_{22}^*}{1 - |S_{22}|^2} = , \quad r_L = \frac{|S_{12}S_{21}|}{1 - |S_{22}|^2}$$

This can be analyzed in the following order.

1) $1/\Gamma_L = e^{j\theta}$; a unit circle for which only the sign of the phase changes.
2) $-1/\Gamma_L = e^{+j\pi + j\theta}\sqrt{2}$; a unit circle for which the phase changing by 180°.
3) $S_{22} - 1/\Gamma_L$ a unit circle with center S_{22}
4) The nearest distance from the origin to the center of the locus of $1/(S_{22} - 1/\Gamma_L)$ is given by the following.

$$\frac{S_{22}^*}{|S_{22}|}, \quad \frac{1}{|S_{22}| + 1}, \quad \frac{1}{|S_{22}| - 1}$$

With these, the locus can be found in the same way.

8.8 Stability is achieved when the locus above is in the unit circle in the Γ_{in} plane; obtain the necessary and sufficient condition for stability from this condition.